SCAT
SCIENTIFIC COMPUTING ADVANCED TRAINING

ALFA
EUROPEAID
CO-OPERATION OFFICE

First Latin American SCAT Workshop:
Advanced Scientific Computing and Applications

Microfluidics

gas-phase flow at the micro-scale

Prof David Emerson

CCLRC Daresbury Laboratory

University of Strathclyde

CCLRC

University of Strathclyde Glasgow

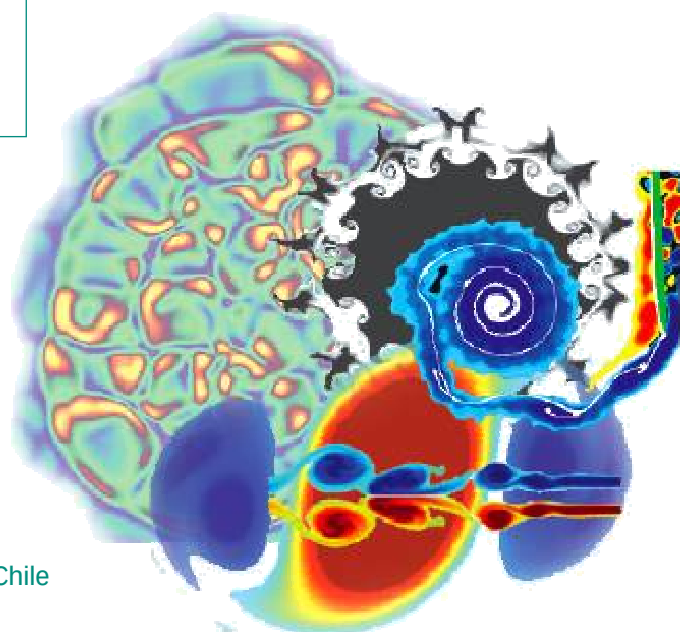

Outline

- Gas dynamics for micro-systems
- The Knudsen number
- Slip flow – boundary treatment
  - Rotating Couette flow
  - Flow past a micro-sphere
  - Oscillating devices
- Transition flow

Introduction to gas flow in MEMS

- Rarefied (or non-equilibrium) gas flows have until recently been associated with low-density applications such as vacuum science and high-altitude applications, such as space vehicle technology.
- However, the advent of Micro-Electro-Mechanical Systems (MEMS) has opened up an entirely new area of research where non-equilibrium gas behaviour has become very important.
- MEMS can combine electrical, mechanical and fluidic components down to a characteristic length scale of 1 micron i.e. *three orders of magnitude* smaller than conventionally machined components.
- The small dimensions of MEMS imply that non-equilibrium effects are important for gas flows, even under atmospheric pressures.

The Knudsen number Kn

- Kn = λ / L
  - Air at S.A.T.P: mean free path, λ ~ 10^{-7} m
    device length L ~ 10^{-6} m
  - Hence Kn ~ 0.1
  - Rarefaction effects can be appreciable
- What does this imply?
  - Navier Stokes equations in conjunction with no-slip boundary conditions not valid for many gas flows in MEMS
  - Slip-flow boundary conditions are needed
  - Mass flow rates, velocity gradients, wall shear stresses and hydrodynamic drag forces will be affected

Knudsen number classification

- Euler equations (neglecting diffusion): $Kn \to 0$ & $(Re \to \infty)$
- Navier-Stokes equations (no-slip): $Kn \leq 10^{-3}$
- Navier-Stokes equations (slip): $10^{-3} \leq Kn \leq 10^{-1}$
- Transition regime: $10^{-1} \leq Kn \leq 10$
- Free molecular flow: $Kn > 10$ $(\to \infty)$

- (see Schaaf and Chambre, 1961 or Gad-el-Hak, 1999)

Describing the behaviour of a gas

The *Knudsen number* is a convenient way to describe the state of a gas

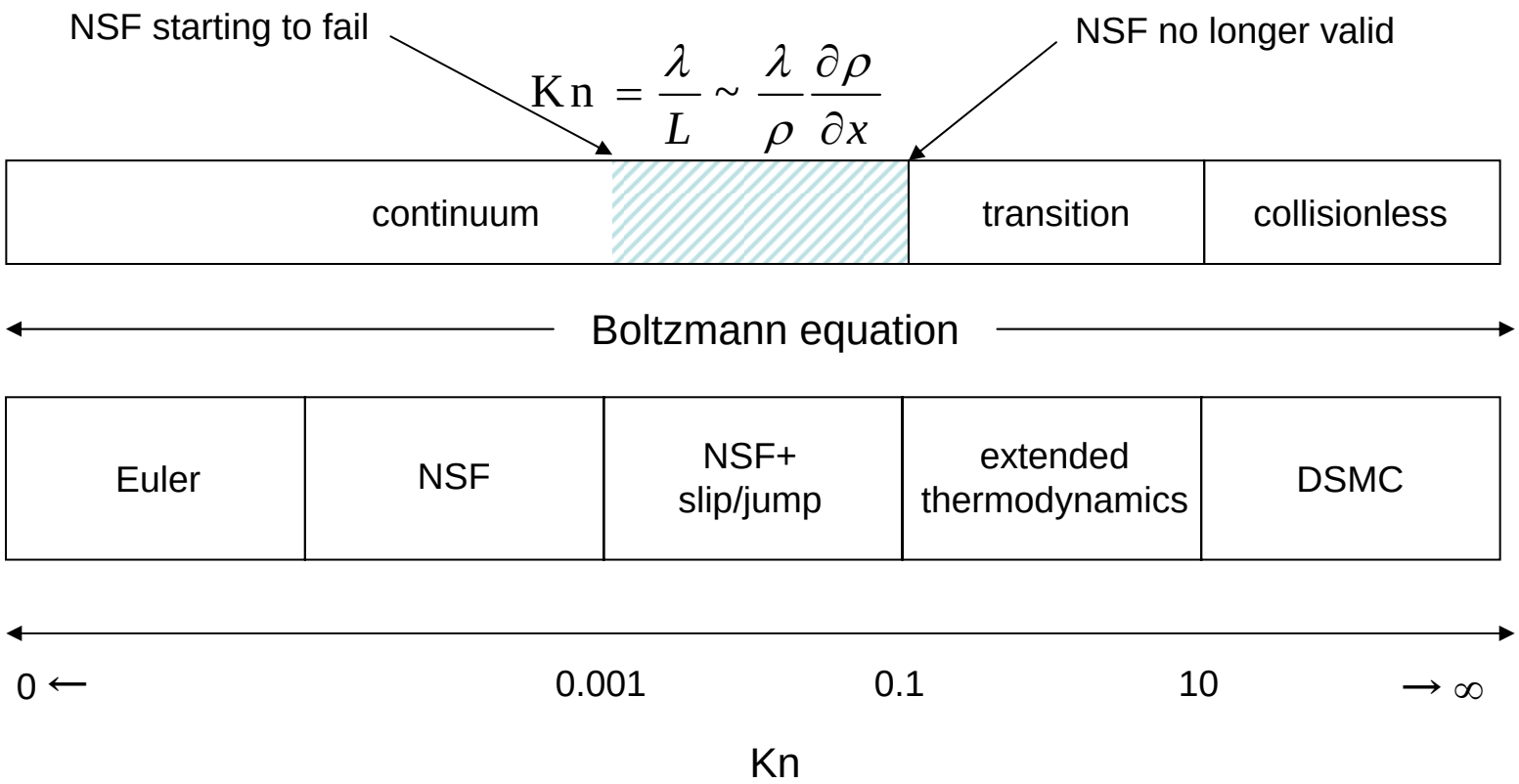

Describing the behaviour of a gas

The *Knudsen number* is a convenient way to describe the state of a gas

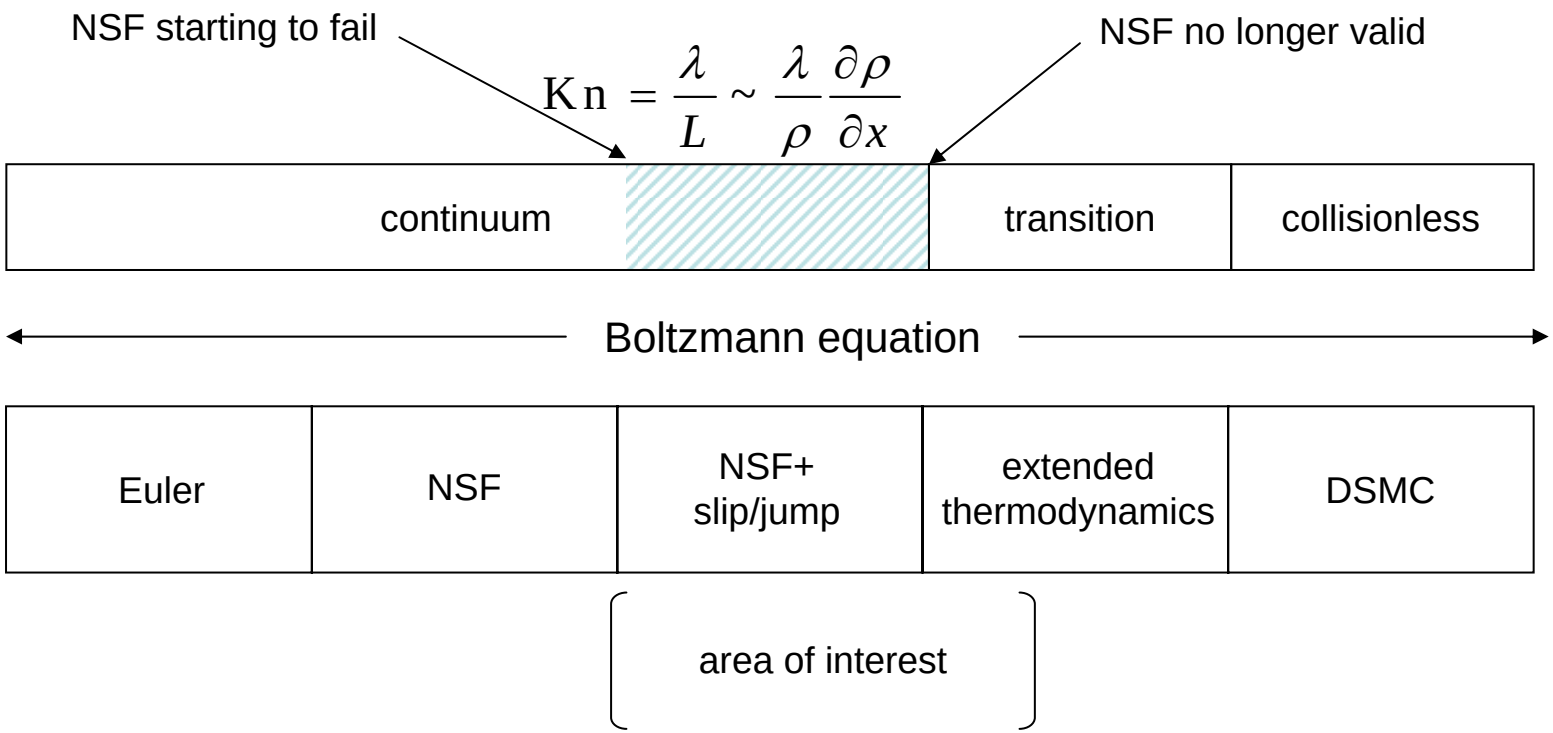

$$0.001 \leq \mathrm{Kn} \approx 1.0$$

Knudsen number – altitude variation

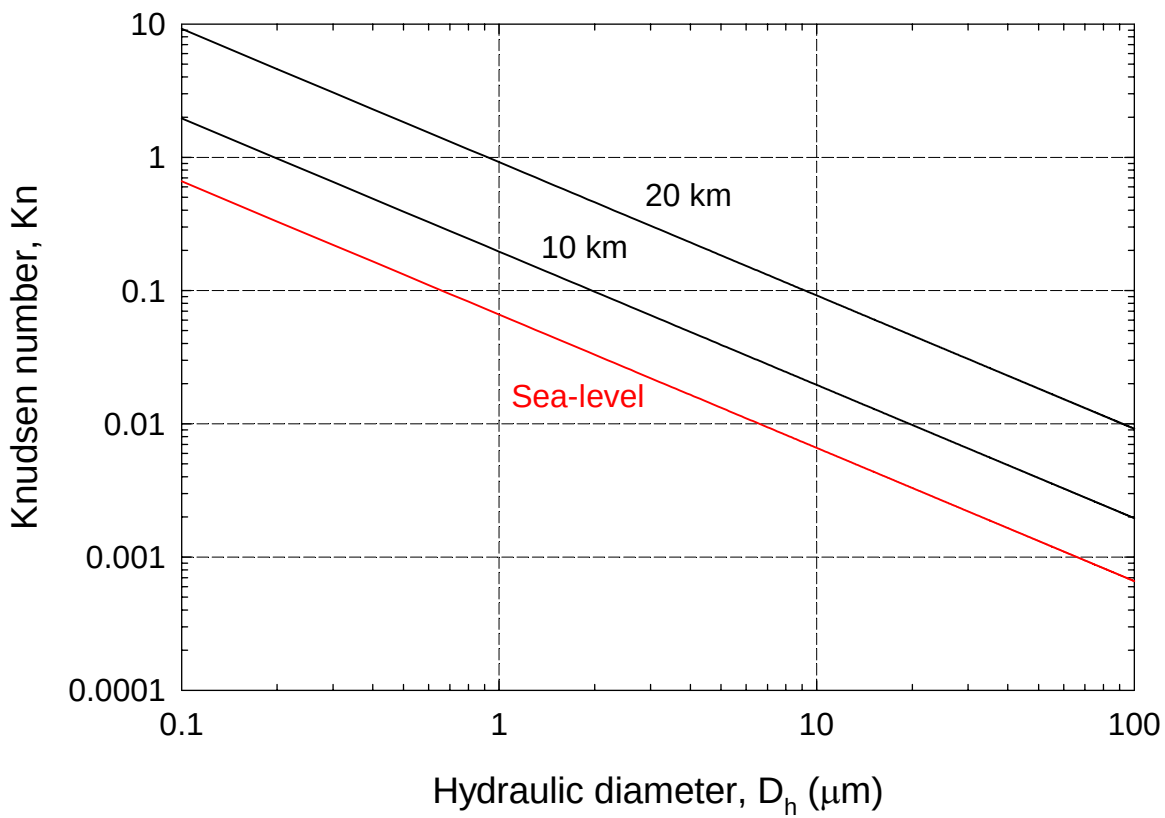

Gas flow in micro-devices

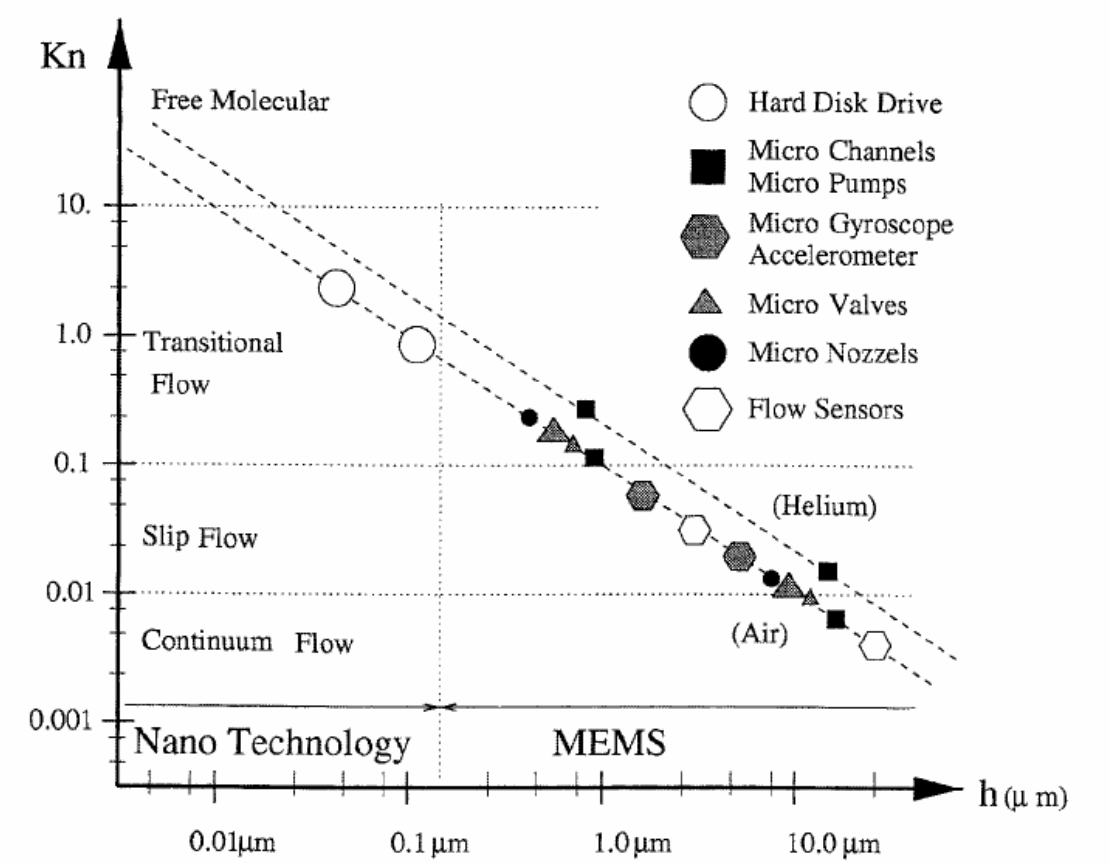

Source: A. Beskok, Numerical Heat Transfer, Part B, 40, 451-471, 2001

Tangential slip-velocity boundary conditions

- Non-equilibrium effects in the slip-flow regime can be taken into account by modifying the boundary treatment at the walls.
- The correct approach was developed by Basset (1888) who proposed that the tangential slip velocity could be modelled using an assumed linear relationship between the shear stress and the slip velocity at the wall:

$$\tau_t = \beta u_t$$

- where τ_t is the tangential shear stress at the wall, u_t is the slip-velocity and β is the slip-coefficient.

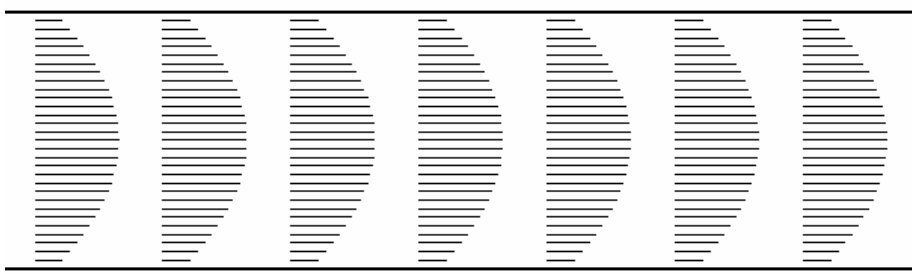

Slip flow between a pair of infinite parallel plates (Kn=0.165)

Tangential slip-velocity boundary conditions

Schaaf & Chambre (1961) demonstrated that Basset's boundary treatment is equivalent to Maxwell's first-order slip velocity equation, provided the slip coefficient, β, is related to the mean free path of the molecules, λ , as follows:

$$\beta = \frac{\mu}{\left(\frac{2-\sigma}{\sigma}\right)\lambda}$$

where μ is the coefficient of viscosity and σ is the tangential momentum accommodation coefficient (TMAC).

The slip velocity at the wall can thus be written as

$$u_t = \frac{\tau_t}{\beta} = \left(\frac{2-\sigma}{\sigma}\right)\frac{\lambda}{\mu}\tau_t$$

Tangential momentum accommodation coefficient

- The TMAC, σ, defines the proportion of gas molecules reflected diffusively
- For smooth walls: $\sigma \to 0$ and for rough walls: $\sigma = 1$

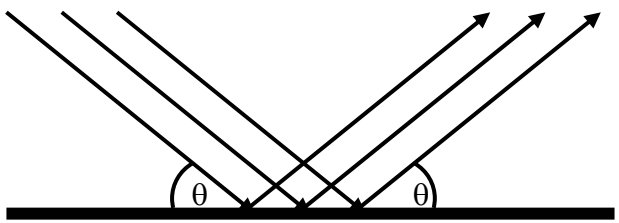

Smooth Wall: Specular Reflection ($\sigma = 0$)

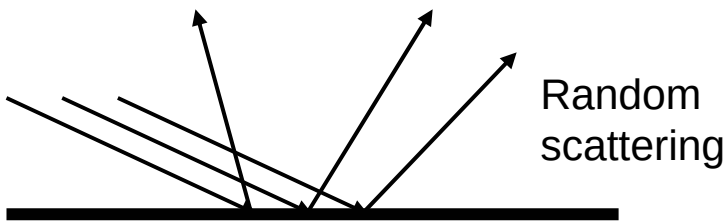

Rough Wall: Diffuse Reflection ($\sigma = 1$)

- Silicon micro-machined components exhibit tangential momentum accommodation coefficients ranging from 0.8 to 1.0 (Arkilic et al., 1997)

Gas flow through micro-channels

Validation against experimental data: flow of helium

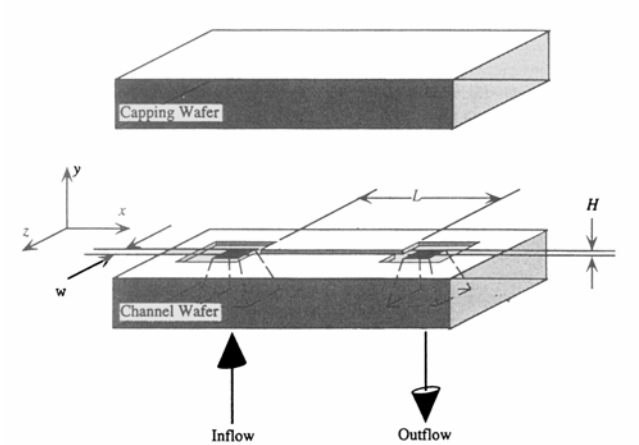

Schematic view of silicon micro-machined channel (Arkilic et al, 1997)

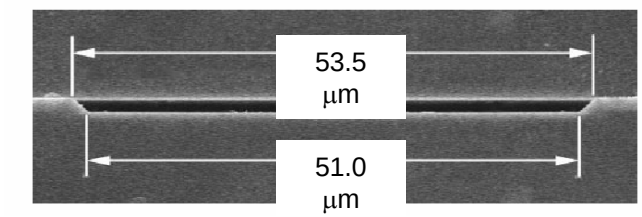

SEM of channel cross section

Parameter	Value
Channel length	7500 μm
Channel width	52 μm
Channel height	1.33 μm
Temperature	314 K
Viscosity	20.66 x 10^{-6} Ns/m^2
Specific gas constant	2077 J/KgK
Collision diameter	210 x 10^{-12} m
Outlet pressure (P_o)	100.8 kPa
Pressure ratio (P_{in} / P_o)	1.2 - 2.6
Outlet Mach number	0.5 - 4 x 10^{-4}
Outlet Kn number	0.165
Outlet mean free path	0.219 μm
Reynolds number	0.5 - 4 x 10^{-3}

Helium mass flow rate through a silicon micro-channel

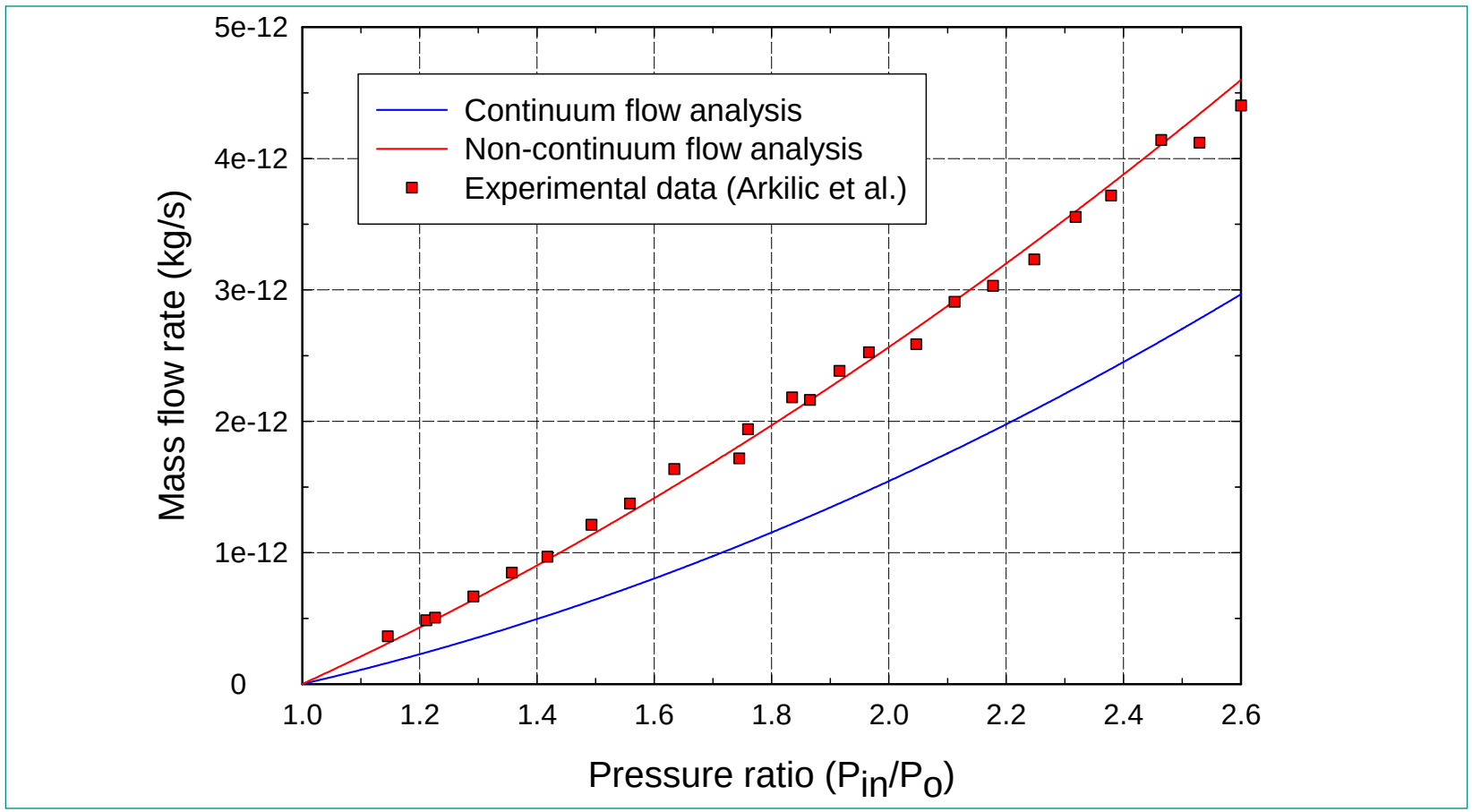

Validation against experiment

- Extending the Navier-Stokes equations into the slip-flow regime ($Kn \leq 10^{-1}$) provides a significant improvement over the continuum (no-slip) approach.
- The Navier-stokes equations (with slip) provide reasonable predictions of the mass-flow rate for Knudsen numbers up to approximately Kn = 0.2.
- There have been numerous experiments considering the mass flow rates through micro-channels e.g. Pfahler *et al*. (1991), Harley *et al*. (1995), Arkilic *et al*. (1997, 2001), Maurer *et al*. (2003). However, to date, no experimental data is available for the velocity profile within the gas.
- There are also questions regarding the extension of the analysis to second-order accuracy in Knudsen number - and how to evaluate the slip velocity at sharp corners of the channel e.g. in a cavity.

Gas flow in micro-bearings

Cylindrical Couette flow

The classic test case of cylindrical Couette flow highlights some important and very non-intuitive behaviour at the micro-scale.

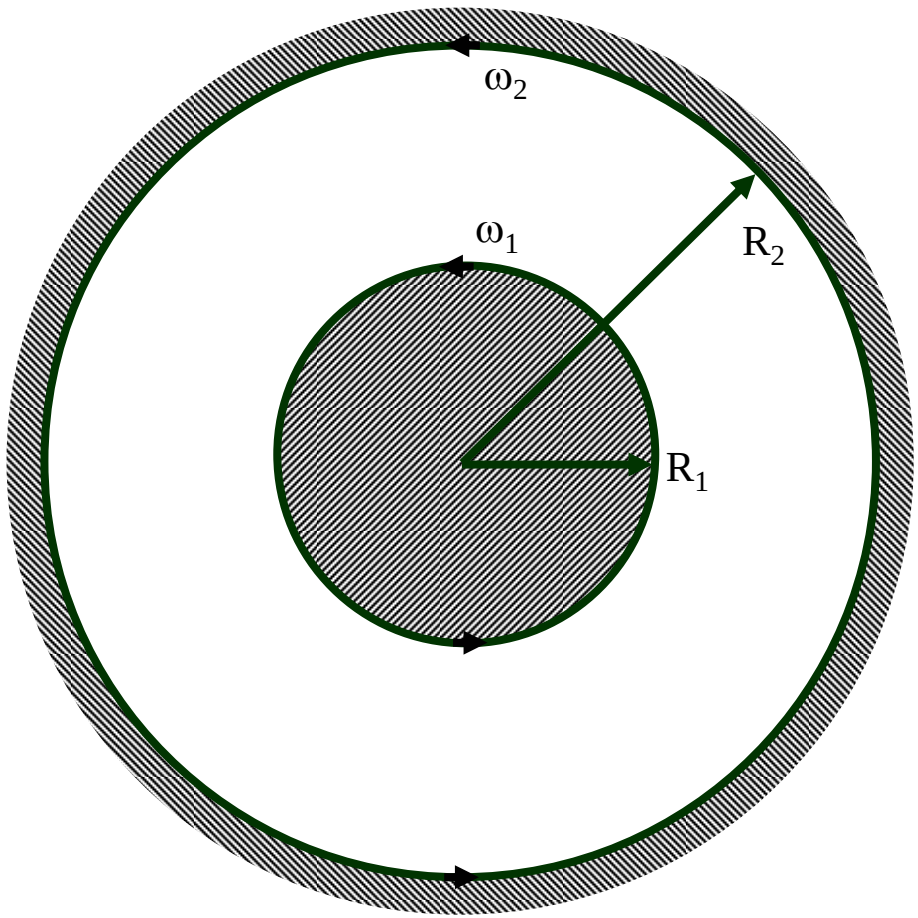

Navier-Stokes solution for rotating Couette flow

In a cylindrical polar co-ordinate (r,θ) reference frame, the tangential momentum expression of the incompressible Navier-Stokes equations for rotating Couette flow can be written as [Schlichting]:

$$\frac{d^2 u_\theta}{dr^2} + \frac{d}{dr}\left(\frac{u_\theta}{r}\right) = 0$$

The general solution for the velocity profile can be written as:

$$u_\theta(r) = ar + \frac{b}{r}$$

$$a = \frac{A\omega_1 - B\omega_2}{A - B} \qquad \text{and} \qquad b = \frac{\omega_1 - \omega_2}{B - A}\,.$$

Rotating Couette flow: Navier-Stokes velocity profile

The interesting solution is when ω_2 is zero i.e. when the outer cylinder is stationary and the inner cylinder is rotating.

$$u_\theta(R_1) = \omega_1 R_1 \quad \text{and} \quad u_\theta(R_2) = 0$$

This allows the values of A and B to be determined:

$$A = \frac{1}{R_2^2} \qquad \text{and} \qquad B = \frac{1}{R_1^2}$$

Velocity field for continuum solution

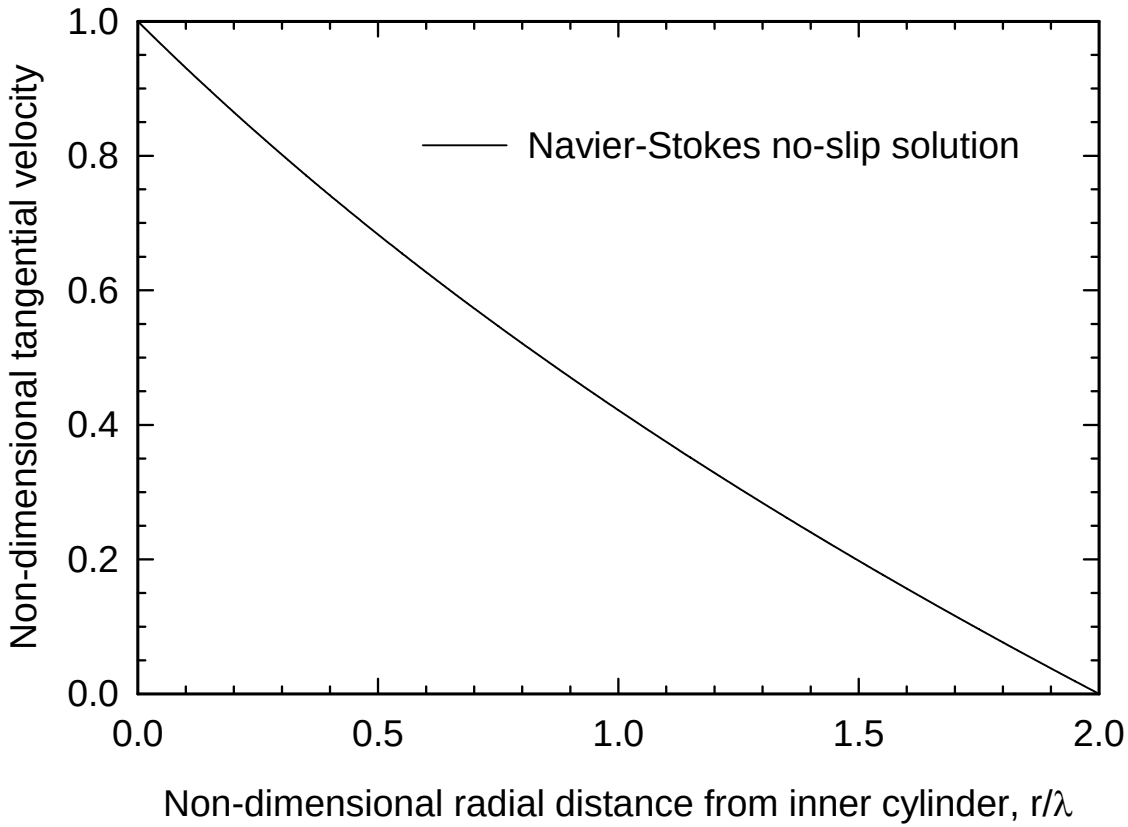

Figure shows the velocity profile that occurs in the continuum flow regime

Rotating Couette flow at the micro-scale

We follow the same process with $\omega_2 = 0$ but the solution now employs Maxwell's slip-velocity boundary condition e.g.

$$u_\theta(R_1) = \omega_1 R_1 + \frac{(2-\sigma_1)}{\sigma_1}\lambda\left(\frac{du_\theta}{dr} - \frac{u_\theta}{r}\right)\Bigg|_{r=R_1}$$

$$u_\theta(R_2) = \cancel{\omega_2 R_2} - \frac{(2-\sigma_2)}{\sigma_2}\lambda\left(\frac{du_\theta}{dr} - \frac{u_\theta}{r}\right)\Bigg|_{r=R_2}$$

$\omega_2 = 0$

The values of A and B are now given by:

$$A = \frac{1}{R_2^2}\left(1 - \frac{(2-\sigma_2)}{\sigma_2}\frac{2\lambda}{R_2}\right) \quad \text{and} \quad B = \frac{1}{R_1^2}\left(1 + \frac{(2-\sigma_1)}{\sigma_1}\frac{2\lambda}{R_1}\right).$$

Velocity field for micro-scale solution

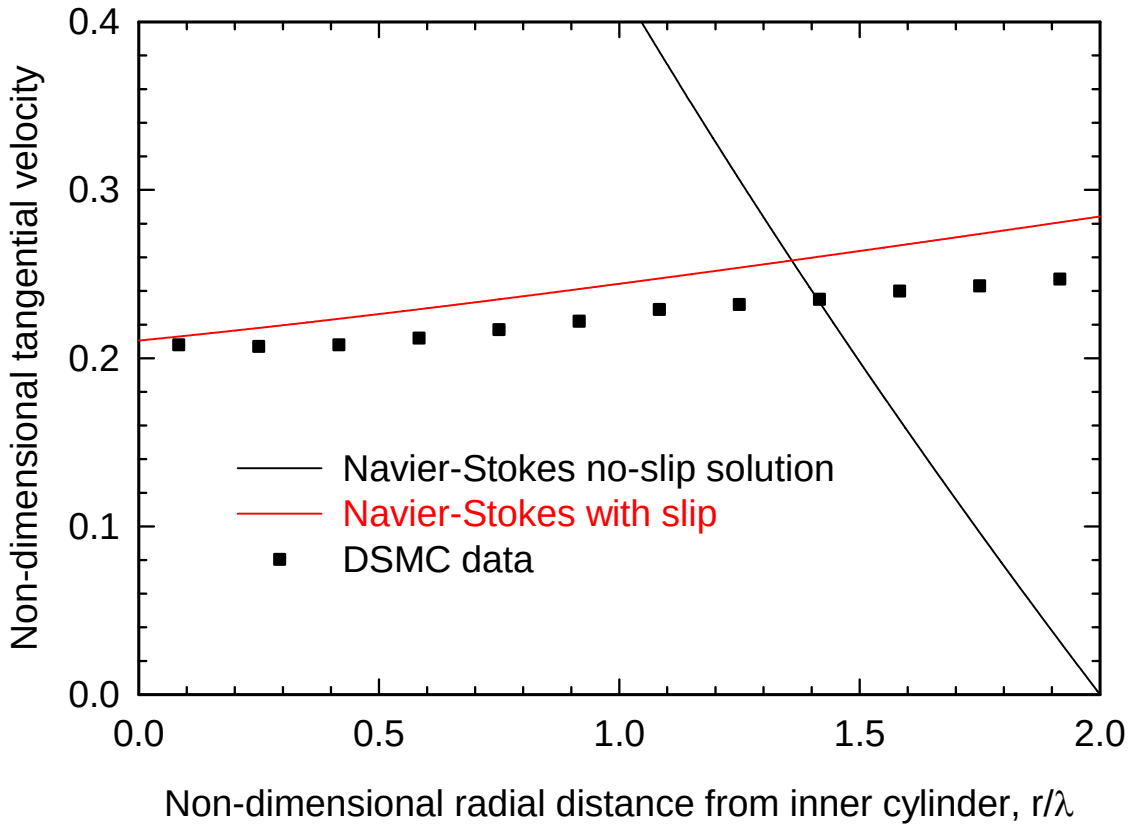

Figure shows an inverted velocity profile that can occur at the micro-scale

Caveat: slip-flow over curved surfaces

Correct slip b.c. $u_\theta(R_1) = \omega_1 R_1 + \frac{(2-\sigma_1)}{\sigma_1}\lambda\left(\frac{du_\theta}{dr} - \frac{u_\theta}{r}\right)\Big|_{r=R_1}$

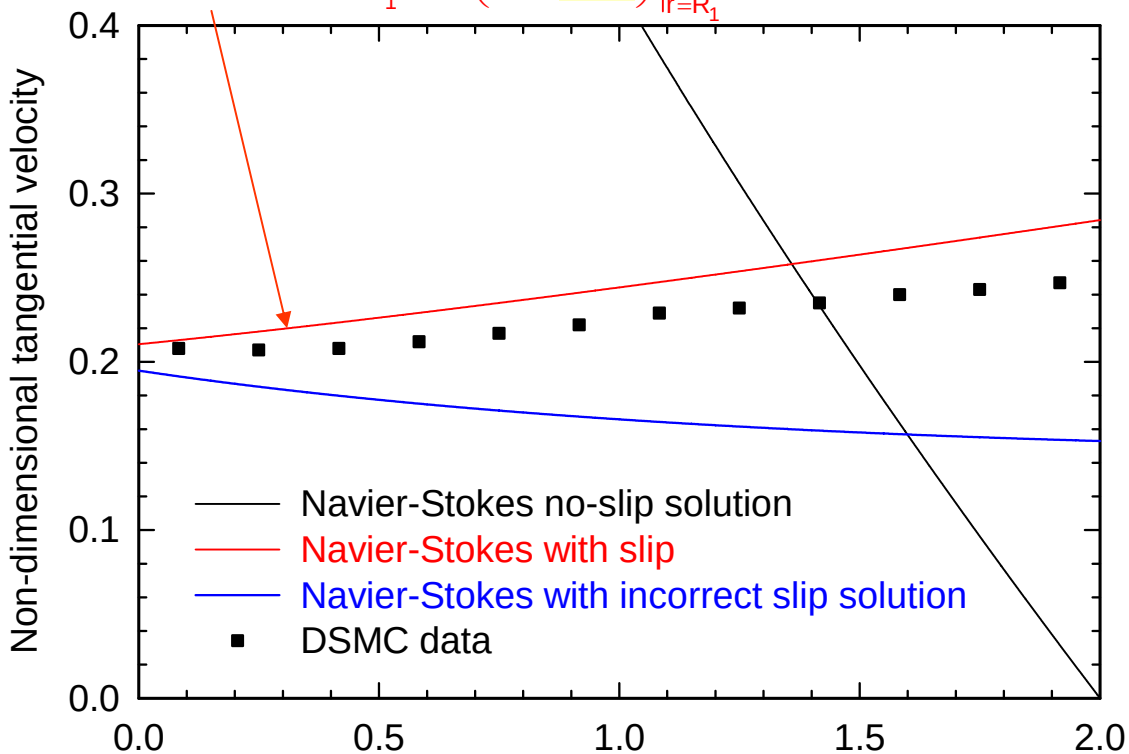

Figure shows the effect of not including the u_θ / r term in the velocity derivative

Caveat: slip-flow over curved surfaces

Correct slip b.c. $u_\theta(R_1) = \omega_1 R_1 + \frac{(2-\sigma_1)}{\sigma_1}\lambda\left(\frac{du_\theta}{dr} - \frac{u_\theta}{r}\right)\Big|_{r=R_1}$

Incorrect slip b.c. $u_\theta(R_1) = \omega_1 R_1 + \frac{(2-\sigma_1)}{\sigma_1}\lambda\frac{du_\theta}{dr}\Big|_{r=R_1}$

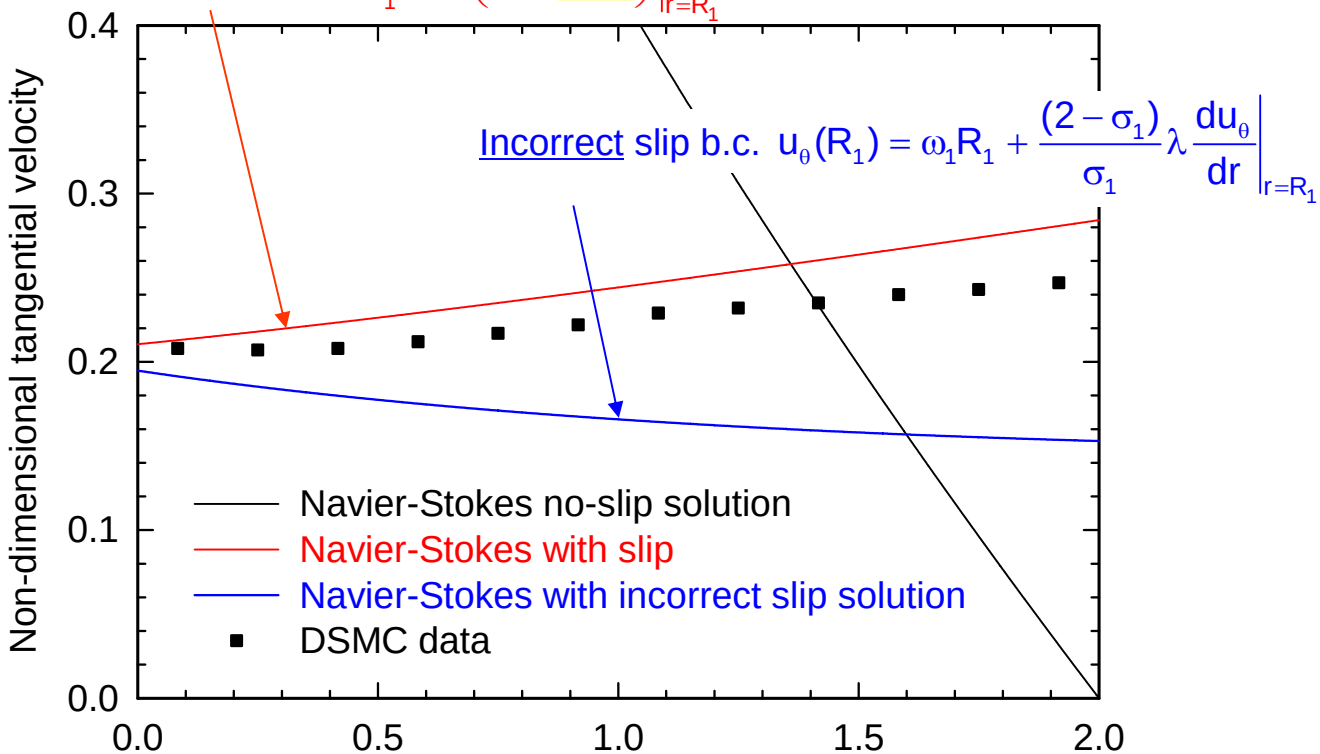

Figure shows the effect of not including the u_θ / r term in the velocity derivative

Comparison against DSMC data

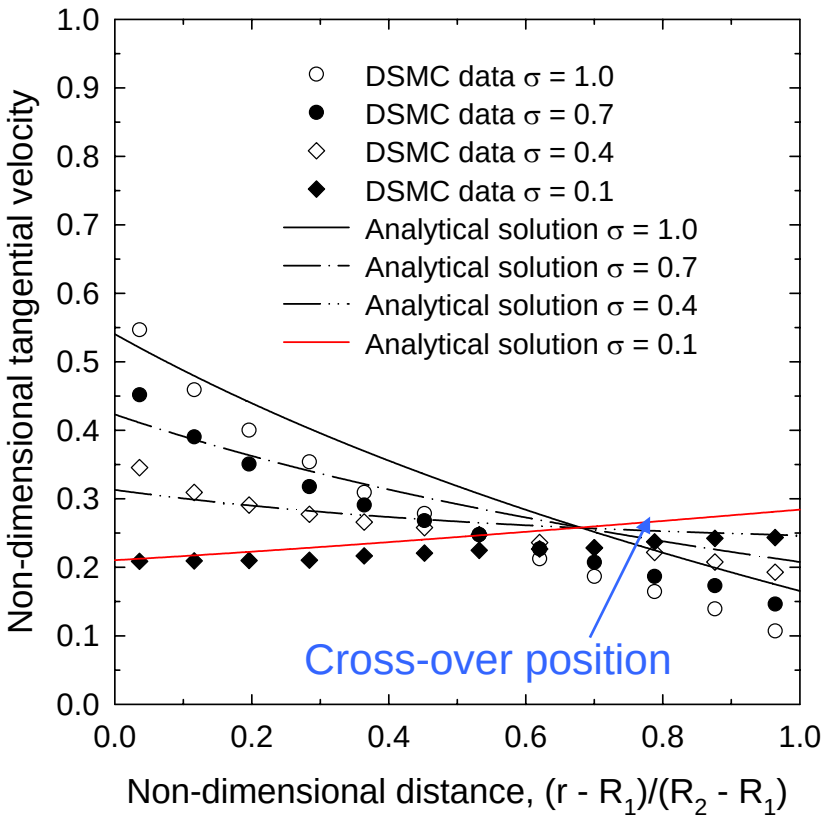

$$R_1 = 3\lambda \text{ and } R_2 = 5\lambda$$

$$\omega_1 = 5.17 \times 10^8 \, \text{rad s}^{-1}$$

$$\lambda = 6.25 \times 10^{-8} \, \text{m}$$

$$\text{Kn} = 0.5$$

Source of DSMC data:

K.W. Tibbs, F. Baras and A.L. Garcia, "Anomalous flow profile due to the curvature effect on slip length", *Phys. Rev. E* **56**, pp. 2282-2283, 1997.

Cross-over position

The family of velocity profiles in the previous figure pass through a common point that is *independent* of the value of the TMAC. Using the Navier-Stokes equations, it can be shown that the cross-over point occurs at:

$$r = \sqrt{\frac{R_1^3 + R_2^3}{R_1 + R_2}}$$

For the current problem ($R_1=3\lambda$ and $R_2=5\lambda$), this location is at $r/\lambda = \sqrt{19}$ The DSMC data show the same phenomenon although the location and velocity magnitude is slightly different.

Impact of the TMAC on the velocity profile

The criterion for the occurrence of a *fully-inverted* velocity profile can be shown to be:

$$\sigma_2 < 2\left(1+\frac{\left(R_1^2+R_2^2\right)R_2}{2\lambda R_1^2}\right)^{-1}$$

while, the criterion for the occurrence of a partially-inverted velocity profile can be shown to be:

$$2\left(1+\frac{\left(R_1^2+R_2^2\right)R_2}{2\lambda R_1^2}\right)^{-1} < \sigma_2 < 2\left(1+\frac{R_2}{\lambda}\right)^{-1}$$

NB: The inversion only comes from the TMAC at the outer cylinder.

Limiting cases

An interesting solution can be obtained for $\sigma_1 = 1$ and $\sigma_2 \to 0$

The *non-dimensionalised* velocity profile is: $$\frac{u_\theta(r)}{\omega_1 R_1} \to \frac{r}{R_1}$$

i.e. at the inner wall, the gas exhibits no-slip whilst at the outer wall the velocity exceeds the driving velocity by the factor R_2/R_1

This is a very non-intuitive result that has now been backed up by DSMC.

Comparison against DSMC data

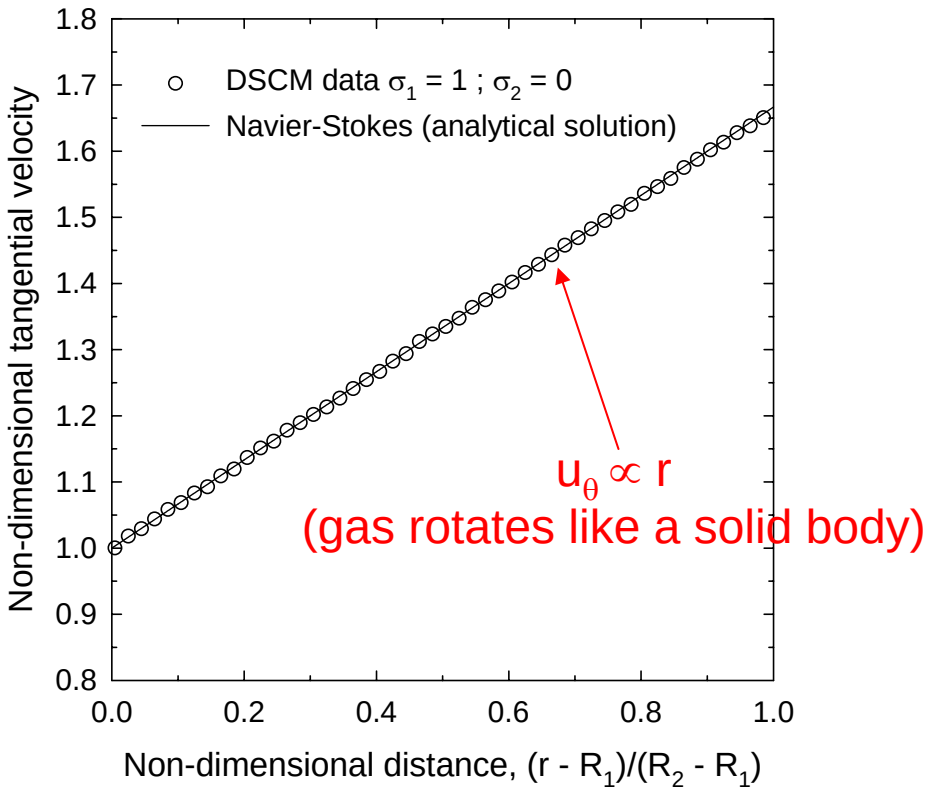

$u_\theta \propto r$

(gas rotates like a solid body)

$R_1 = 3\lambda$ and $R_2 = 5\lambda$

$\omega_1 = 5.17 \times 10^8 \, \text{rad s}^{-1}$

$\lambda = 6.25 \times 10^{-8} \, \text{m}$

$\text{Kn} = 0.5$

$\sigma_1 = 1 \; ; \; \sigma_2 = 0$

i.e. specular reflection on outer cylinder

DSMC data courtesy of Prof. Stefan Stefanov, Dept. of Complex and Multiphase Flows, Institute of Mechanics, Sofia, Bulgaria

The system is shear-free for $\sigma_2 = 0$ and is in agreement with DSMC predictions.

Comparison against DSMC data: effect of varying σ_2

$\sigma_1 = 1$

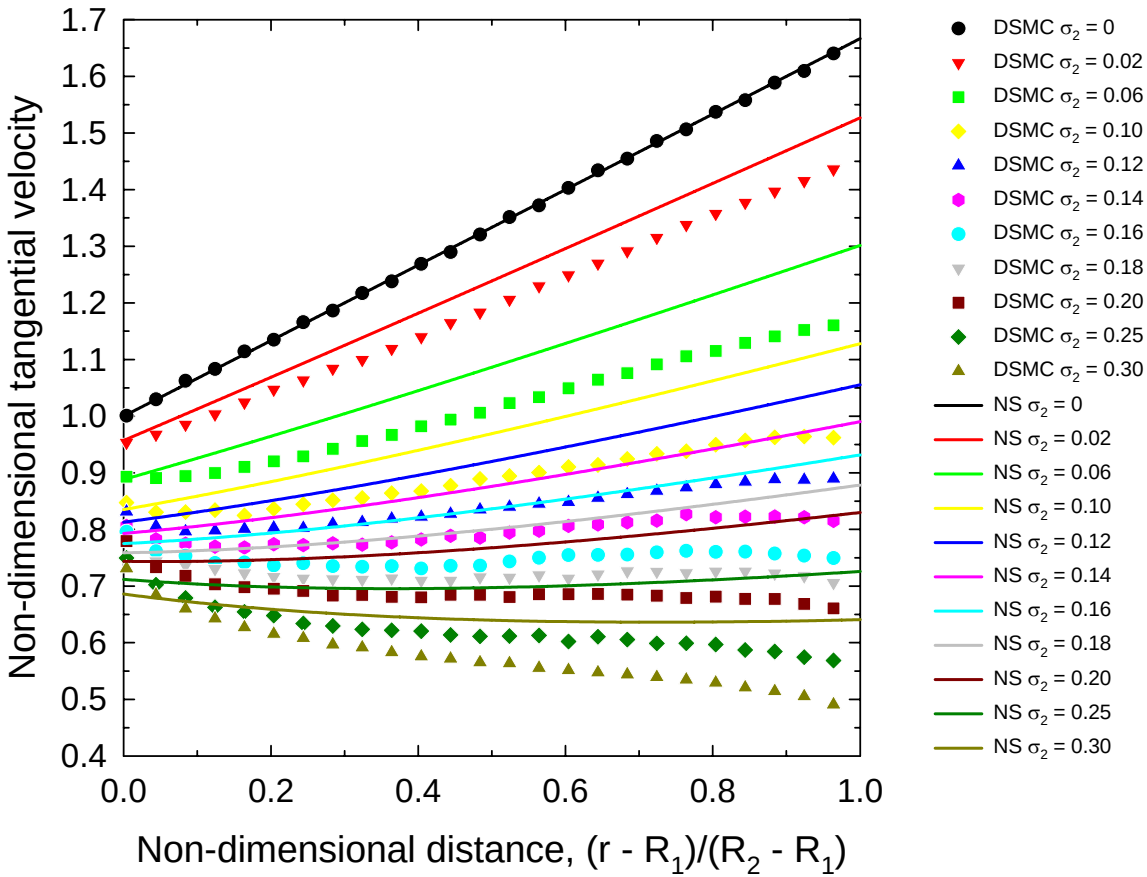

DSMC data courtesy of Prof. Stefan Stefanov, Dept. of Complex and Multiphase Flows, Institute of Mechanics, Sofia, Bulgaria

Flow past an unconfined micro-sphere

Stokes' 1st problem

Isothermal slip flow past an unconfined sphere

- Isothermal *slip flow* past an unconfined sphere at very low Reynolds and Mach numbers was first analysed by Basset (1888) using Stokes' creeping flow approximation.
- In continuum (no-slip) flows, it can be shown that the normal stress must vanish along any rigid no-slip impermeable boundary.
- In contrast, the tangential slip boundary condition associated with microflows generates a normal stress term that causes *an additional force on the sphere*.
- The total drag force (D_T) is therefore composed of three separate components, namely:
  - skin friction drag (D_S)
  - pressure (or form) drag (D_P)
  - normal stress drag (D_N).

$$D_T = D_S + D_P + D_N$$

Example of tangential slip-velocity boundary condition

Consider axisymmetric flow past an unconfined sphere:

In spherical coordinates, the shear stress on the sphere can be found from:

$$\tau_{r\theta} = \mu\left(\frac{\partial u_\theta}{\partial r} - \frac{1}{r}u_\theta + \frac{1}{r}\frac{\partial u_r}{\partial \theta}\right)$$

=0 on surface of sphere

Hence, the slip-velocity boundary condition can be expressed as:

$$u_\theta\big|_{r=a} = \left(\frac{2-\sigma}{\sigma}\right)\frac{\lambda}{\mu}\tau_{r\theta} = \frac{2-\sigma}{\sigma}\lambda\left(\frac{\partial u_\theta}{\partial r} - \frac{1}{r}u_\theta\right)\Bigg|_{r=a}$$

Many flow models implementing Maxwell's slip velocity treatment fail to account for this term

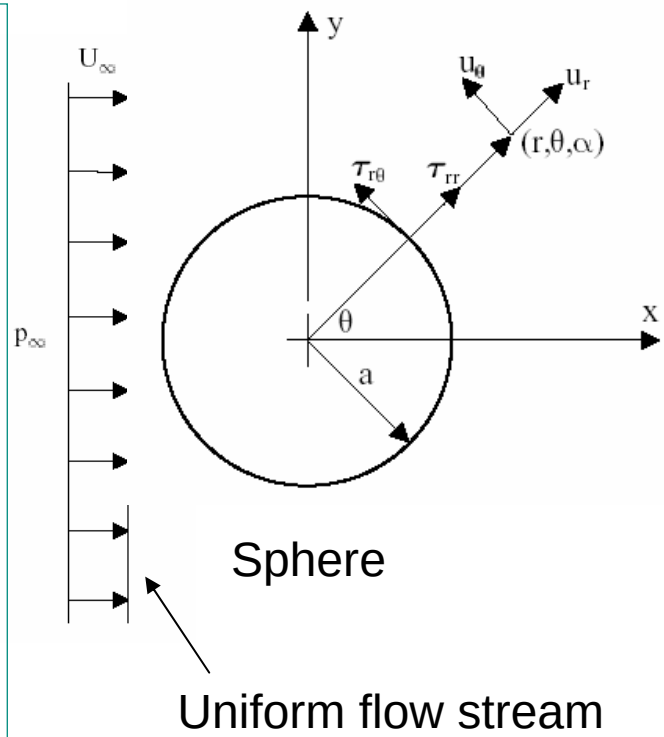

Basset's slip-flow solution for flow past a sphere

$$\text{Skin-friction drag, } D_S = 4\pi\mu Ua \Big/ \left(1+3\frac{(2-\sigma)}{\sigma}Kn\right)$$

$$\text{Pressure drag, } D_P = 2\pi\mu Ua\left(1+2\frac{(2-\sigma)}{\sigma}Kn\right)\Big/\left(1+3\frac{(2-\sigma)}{\sigma}Kn\right)$$

$$\text{Normal stress drag, } D_N = 4\pi\mu Ua\left(2\frac{(2-\sigma)}{\sigma}Kn\right)\Big/\left(1+3\frac{(2-\sigma)}{\sigma}Kn\right)$$

$$\text{Total drag, } D_T = 6\pi\mu Ua\left(1+2\frac{(2-\sigma)}{\sigma}Kn\right)\Big/\left(1+3\frac{(2-\sigma)}{\sigma}Kn\right)$$

Stokes' original drag equation is recovered as $Kn \to 0$

where $Kn = \frac{\lambda}{a}$

Comparison of non-dimensionalised drag force

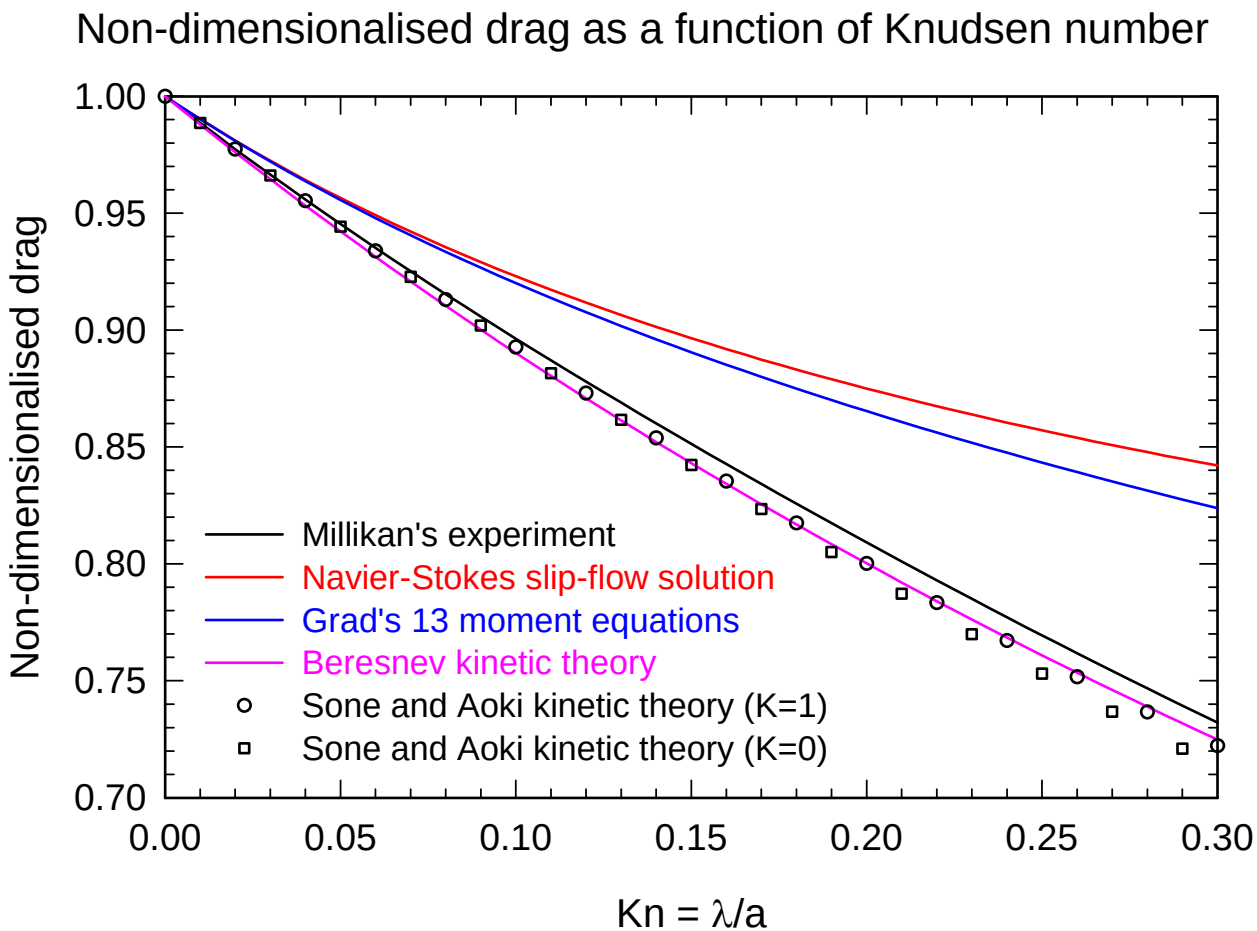

Effect of omitting u_θ / r for flow past an unconfined sphere

Predicted drag on an unconfined sphere ($\sigma = 0.1$)

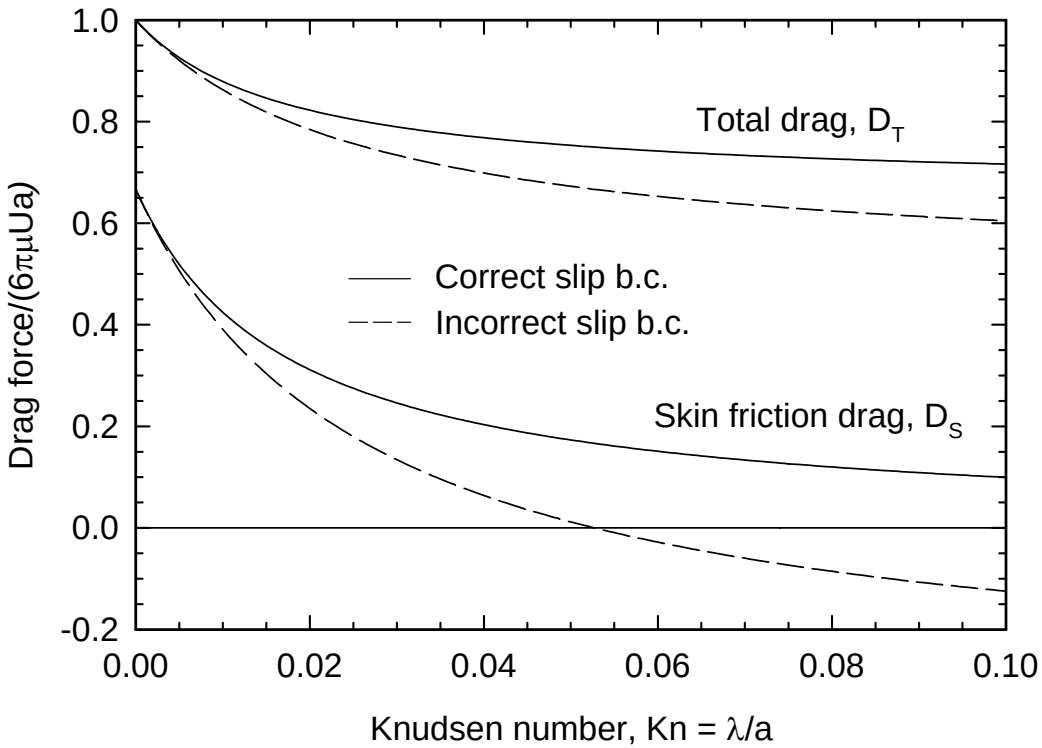

Source: R.W. Barber, Y. Sun, X.J. Gu, D.R. Emerson, "Isothermal slip flow over curved surfaces", *Vacuum*, 76(1), pp. 73-81, 2004.

Are quantum effects important - revisited

- We know that Newton's second law breaks down under certain conditions which means that the Navier-Stokes equations are no longer appropriate. For gases, the Knudsen number guides us. There are two other areas where Newton's laws are no longer appropriate: one case concerns special relativity which is not an issue for MEMS. The other case is quantum theory.
- Quantum effects are important when a particle's *de Broglie* wavelength is comparable to a typical length scale of the system:

$$\lambda = \frac{h}{p} = \frac{h}{mv}$$

where *h* is Planck's constant, *p* is the particle's momentum, which for nonrelativistic gases moving at ~500 m/s, gives λ = 0.2Å.

Drag of sphere in the free-molecular regime

- Previously, we found that quantum effects are not important unless the length scale was very small – what about in the high Kn range?
- In the free-molecular regime, Kn $\rightarrow \infty$ i.e. the mean free path becomes very large.
- Recently, a paper by Drosdoff et al. has shown that quantum mechanical diffraction scattering theory is needed for ultra-dilute gases where the mean free path of a gas molecule is large compared to the sphere radius. A substantial change in the drag force was obtained.

Limitations of the Navier-Stokes equations for gas microflows

- Extending the Navier-Stokes equations into the slip-flow regime ($Kn \leq 10^{-1}$) provides a significant improvement over the continuum (no-slip) approach.
- However, it has been shown that the drag predictions in the slip-flow regime quickly deviate from the experimental data when the Knudsen number approaches 10^{-1}.
- On the other hand, results derived from kinetic theory agree reasonably well with experimental observations over the whole Knudsen number regime.
- We need to develop ways of extending beyond the slip-flow regime.

Developing boundary conditions for planar channel flow

A number of experiments have been conducted that consider the mass flow rates through micro-channels

- Pfahler *et al*. (1991)
- Harley *et al*. (1995)
- Arkilic *et al*. (1997, 2001)
- Lalonde *et al*. (2001)
- Maurer *et al*. (2003)

These investigations have confirmed that the NSF equations must be modified to account for velocity-slip at the wall.

New experimental work underway with Gilbert Meolans group in France

The experimental work has been complemented by theoretical studies of 1st and 2nd order treatment at the solid boundary

$$u_s - u_w = \pm A_1 \frac{\partial u}{\partial y} - A_2 \frac{\partial^2 u}{\partial y^2}$$

$$A_1 = \alpha \left(\frac{2-\sigma}{\sigma} \right) \lambda$$

The evaluation of A_1 remains a problem. Following Maxwell, α is unity, but from kinetic theory, α = 1.146. It arises from the velocity defect and clearly affects the value of the TMAC (σ) and also A_2

Planar channel flow: 2nd order & difficulties

The table illustrates the problem of choosing the "correct" value for A_2

$$u_s - u_w = \pm A_1 \frac{\partial u}{\partial y} - A_2 \frac{\partial^2 u}{\partial y^2}$$

D.A. Lockerby, J.M. Reese, D.R. Emerson and R.W. Barber, "The velocity boundary condition at solid walls in rarefied gas calculations", *Phys. Rev E,* Vol. 69(6), 2004.

See also R.W. Barber and D.R. Emerson, "Challenges in modeling gas-phase flow in microchannels: from slip to transition.", Heat Transfer Engineering, V27 (4): 3-12, 2006

Lang	1.432	T
Schamberg	1.31	T
Deissler	1.125	T
Cercignani	0.98	T
Hadjiconstantinou	0.31	T
Maurer *et al*.	0.23-0.26	E
Lockerby *et al*.	0.19	T
Sreekanth	0.14	E
Beskok & Karniadakis	-0.5	T

Example of theoretical treatment for 2nd order

Extension of the slip-velocity boundary treatment to second-order accuracy. Various formulations are reported in the literature:

$$u\big|_{z=0} = U_{wall} + \frac{2-\sigma}{\sigma}\lambda\left.\frac{\partial u}{\partial z}\right|_{z=0} - \frac{9}{16}\lambda^2\left[2\left.\frac{\partial^2 u}{\partial z^2}\right|_{z=0} + \left.\frac{\partial^2 u}{\partial x^2}\right|_{z=0} + \left.\frac{\partial^2 u}{\partial y^2}\right|_{z=0}\right]$$

(Deissler, Aubert and Colin)

An alternative approach would be to employ the stress tensor from higher-order constitutive relations (e.g. Burnett equations) so that the analysis is locally second-order in Kn. This is discussed in the following paper:

D.A. Lockerby, J.M. Reese, D.R. Emerson and R.W. Barber, "The velocity boundary condition at solid walls in rarefied gas calculations", in *Phys. Rev E,* Vol. 70 017303, 2004.

$$\vec{u}_{slip} = u_{wall} + \frac{(2-\sigma)}{\sigma}\frac{\lambda}{\mu}\vec{\tau}_x - \frac{3}{4}\frac{(\gamma-1)}{\gamma}\frac{Pr}{p}q_x^{MB}$$

$$q_x^{MB} = \frac{\mu^2}{8\rho}\left[(61-45\gamma)\frac{\partial^2 u}{\partial x^2} + (49-45\gamma)\frac{\partial^2 v}{\partial x \partial n} + (49-45\gamma)\frac{\partial^2 w}{\partial x \partial z} + 12\frac{\partial^2 u}{\partial n^2} + 12\frac{\partial^2 u}{\partial z^2}\right]$$

The Knudsen layer

All analyses so far have assumed that the linear stress/strain relationship of the NSF equations holds throughout the domain.

The Knudsen layer forms a nonlinear region close to the wall ~ 1 mean free path thick. It has a dramatic effect on the flow.

2nd order approaches only capture the increased mass flow rate because the slip-velocity is ***increased***.

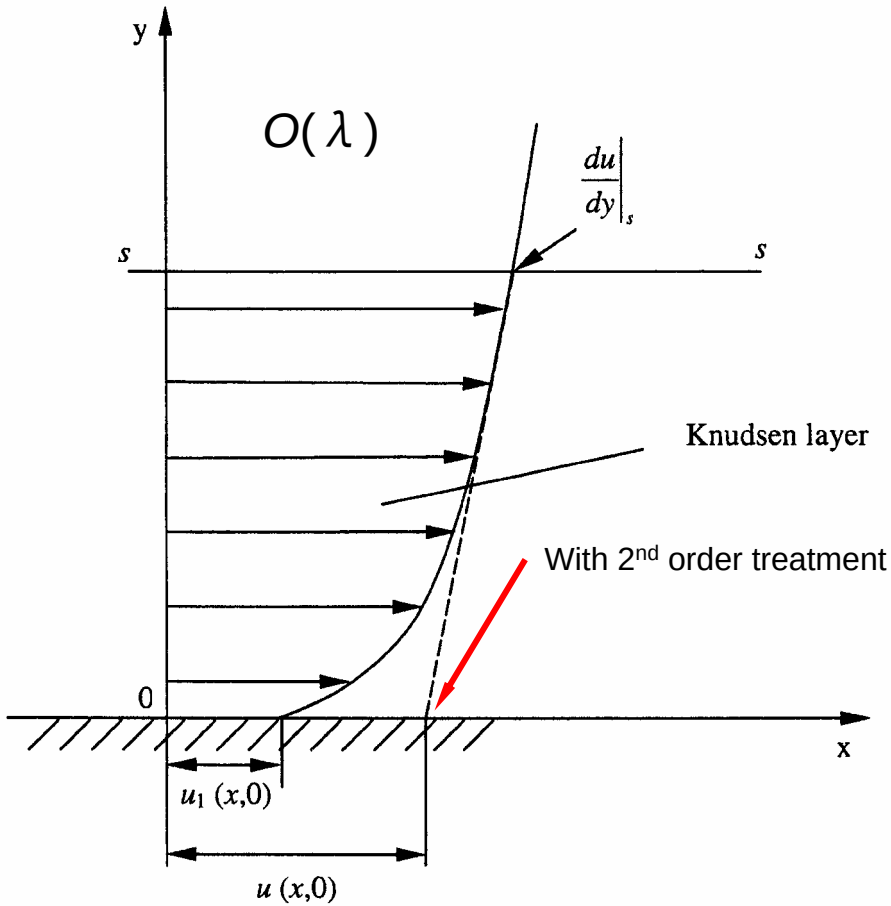

A further issue for gaseous transport in MEMS

The figure shows an updated version of a plot (for air) developed by Bird.

The shaded region is the limit for where the NSF equations can be safely applied. Below that line thermodynamic equilibrium breaks down, followed by the continuum assumption.

Potentially, there are real problems for MEMS.

δ = mean intermolecular spacing

d = mean molecular diameter $(4.1 \times 10^{-10}$ m)

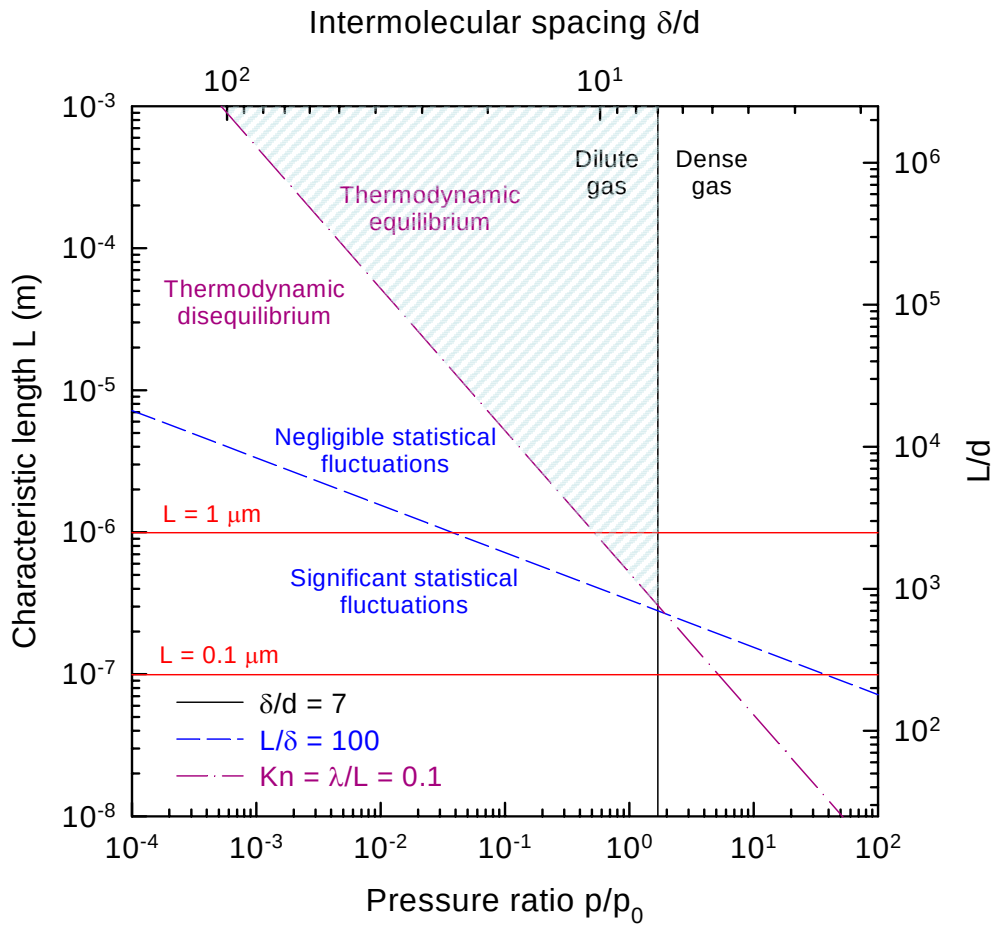

Moving beyond the NSF equations

Boltzmann equation

The Boltzmann equation provides the fundamental description of a gas at all values of the Knudsen number, provided

the gas is dilute

only binary collisions take place

$$\frac{\partial f}{\partial t} + \xi_i \cdot \frac{\partial f}{\partial x_i} = J\left(f_1, f_2\right)$$

$$f = f\left(x_1, x_2, x_3, \xi_1, \xi_2, \xi_3, t\right)$$

where *f* is the molecular distribution function and *J* is the collision operator.

This integro-differential equation is difficult to solve. Some good numerical results for Couette and Poiseuille flow (useful to validate codes). Alternative approaches (DSMC) are very poor at low speed and low *Kn*

A possible option: extended thermodynamics

The approach offers a number of advantages:

- continuum formulation retained
- computational cost *similar* to conventional CFD
- globally second-order (or higher) in Knudsen number
- reduces to NSF equations under appropriate conditions

The disadvantages are that:

- equations highly non-linear and often unstable (e.g. Burnett)
- higher-order boundary conditions are required
- extending to complex molecules & thermochemistry unresolved
- precise Knudsen number range often not known

We have recently implemented the R13/R26 moment equations and they are now being tested and evaluated for a range of problems.

Chapman-Enskog expansion

Expand distribution function about a small parameter, ε

$$f = f^{(0)} + \varepsilon f^{(1)} + \varepsilon^2 f^{(2)} + \ldots\ldots\ldots$$

Zeroth-order expansion yields Euler equations

First-order expansion yields NSF equations

Second-order expansion yields Burnett equations

Higher-order expansions yield super-Burnett, augmented Burnett,…….

Viscous stress tensor $\Pi = \Pi^{(0)} + \Pi^{(1)} + \Pi^{(2)} +$

Heat flux vector $Q = Q^{(0)} + Q^{(1)} + Q^{(2)} +$

Method of Moments

Multiply Boltzmann equation by a molecular property, Φ, and integrate over velocity space

$$\frac{\partial}{\partial t}\int \Phi\, f\, d\xi_i + \frac{\partial}{\partial x_i}\int \Phi\, \xi_i\, f\, d\xi_i = I_\Phi = 0$$

i.e. total mass, momentum, energy are collision invariant.

$\Phi = m \quad \rightarrow$ Conservation of mass

$\Phi = m\xi_i \quad \rightarrow$ Conservation of momentum etc.

Method of Moments vs Chapman-Enskog

- Chapman-Enskog expansion
  - Advantage: boundary conditions can be specified
  - Disadvantage: high-order derivatives, unstable for short wavelegths
- Grad's Method of Moments
  - Advantage: low-order derivatives
  - Disadvantage: boundary conditions difficult to specify, higher moments appear in truncation

Extended thermodynamics using method of moments

- Recent work has focused on extending the NSF methodology using the regularized 13 & 26 moment equations

- Results to be presented will show there is a significant improvement compared to the NSF method (for slip flow) and gives good results for transition flow ($0.1 \leq Kn \leq \sim 1.0$)

- Two cases will be considered: Couette flow, Poiseuille flow

- Note: no boundary conditions have been developed for confined flow problems. We used DSMC to obtain data to "tune" the boundary conditions

•See XJ Gu and DR Emerson, *A computational strategy for the regularized 13 moment equations with enhanced wall-boundary conditions*, to appear in Journal of Computational Physics

Example of boundary treatment for method of moments

Start by expanding distribution function in Hermite polynomials e.g.

$$f = f_M \sum_{n=0}^{\infty} \frac{1}{n!} a_A^{(n)} H_a^{(n)} = f_M \left(a^{(0)} H^{(0)} + a_i^{(1)} H_i^{(1)} + \frac{1}{2!} a_{ij}^{(2)} H_{ij}^{(2)} + \frac{1}{3!} a_{ijk}^{(3)} H_{ijk}^{(3)} + ... \right)$$

where f_M is the local Maxwellian distribution function.

Basically, require 7 boundary conditions with coefficients i.e.

$$u_{1s} = -\frac{2-\alpha}{\alpha} \beta_u \sqrt{\frac{\pi RT}{2}} \frac{\sigma_{12}}{p_\alpha} - \frac{m_{122}}{2 p_\alpha} - \frac{q_1}{5 p_\alpha}$$

$$p_\alpha = p + \frac{\sigma_{22}}{2} - \frac{30 R_{22} + 7\Delta}{840 RT} - \frac{\phi_{2222}}{24 RT}$$

DSMC used to determine variables and find coefficients

Some results for planar Couette flow - velocity

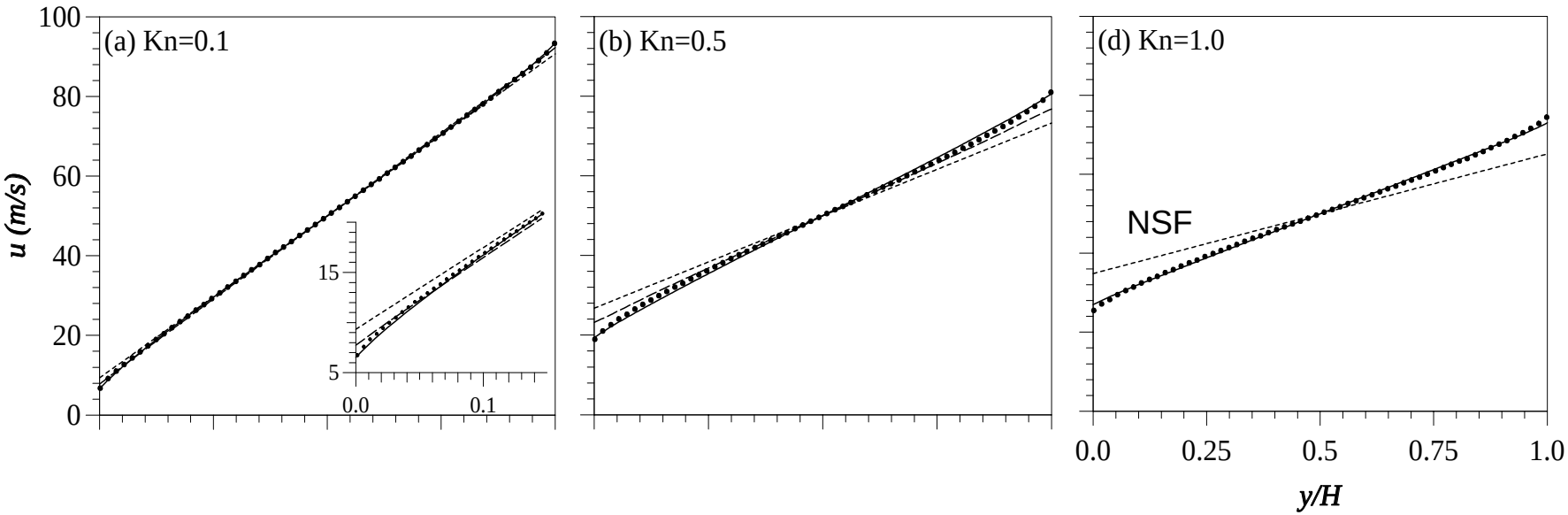

Predicted velocity profiles at a range of Knudsen numbers.

Initial conditions: = 273 *K* and = 100 *m/s*. Symbols DSMC, R26, R13B, NSF

At ~ Kn = 0.75, R13B develops some non-physical wiggles.

Note: R13B does not capture Knudsen layers – profile linear at Kn = 0.5

Some results for planar Couette flow - temperature

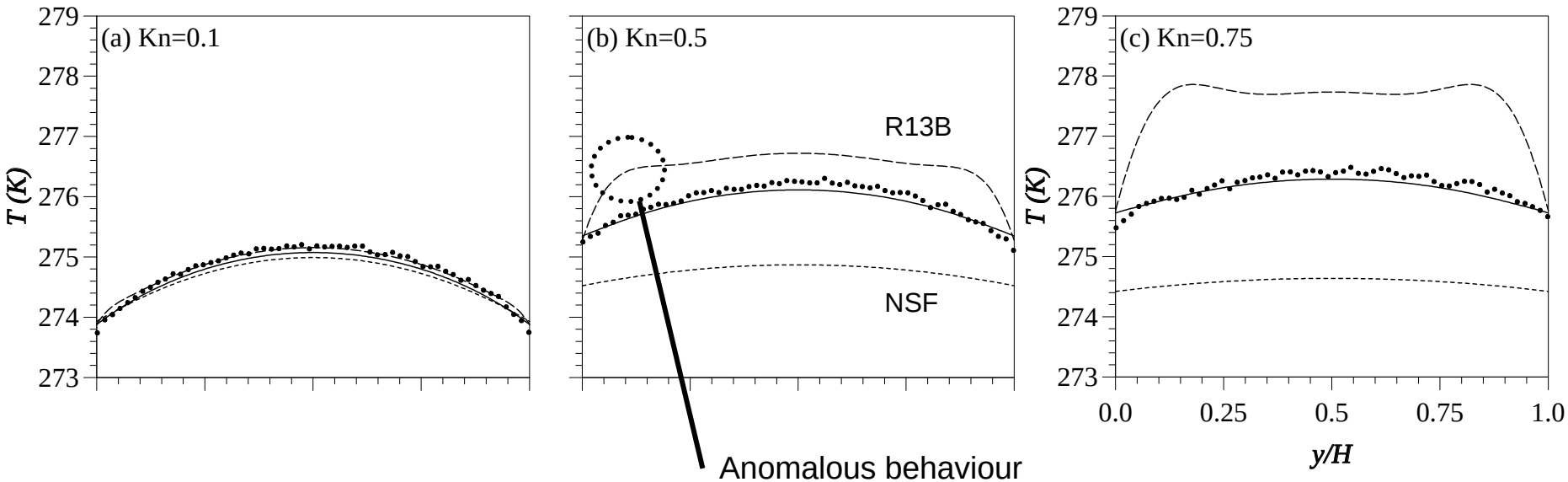

Predicted temperature profiles at a range of Knudsen numbers.

Symbol DSMC, R26, R13B, NSF

NSF always underpredicts. At Kn = 0.5, temperature profile wiggle (feeds back into velocity profile).

Some results for planar Couette flow – heat flux

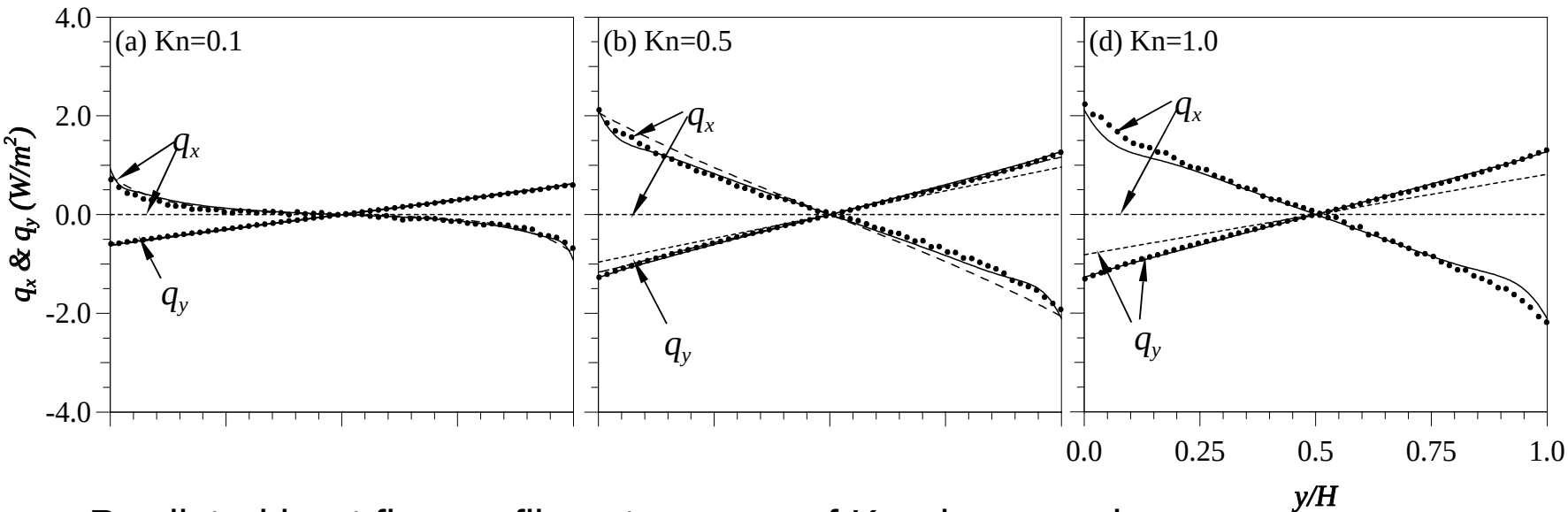

Predicted heat flux profiles at a range of Knudsen numbers.

Symbol DSMC

NSF always predicts zero tangential heat flux. However, nonequilibrium flows exhibit this phenomena *without* a temperature gradient.

At Kn = 1, R26 starts to indicate problems. Similar plots for stress.

Some results for planar Couette flow – velocity-slip

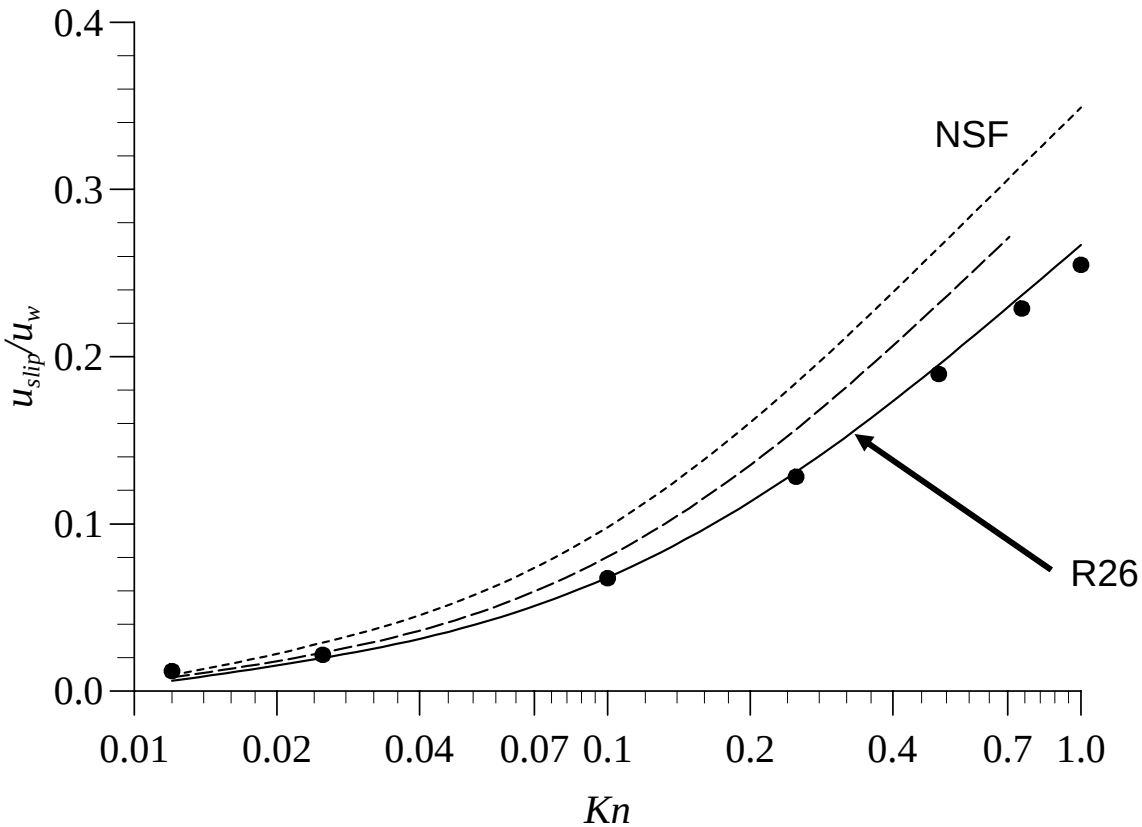

Normalised velocity-slip

Some results for Poiseuille flow – velocity profile

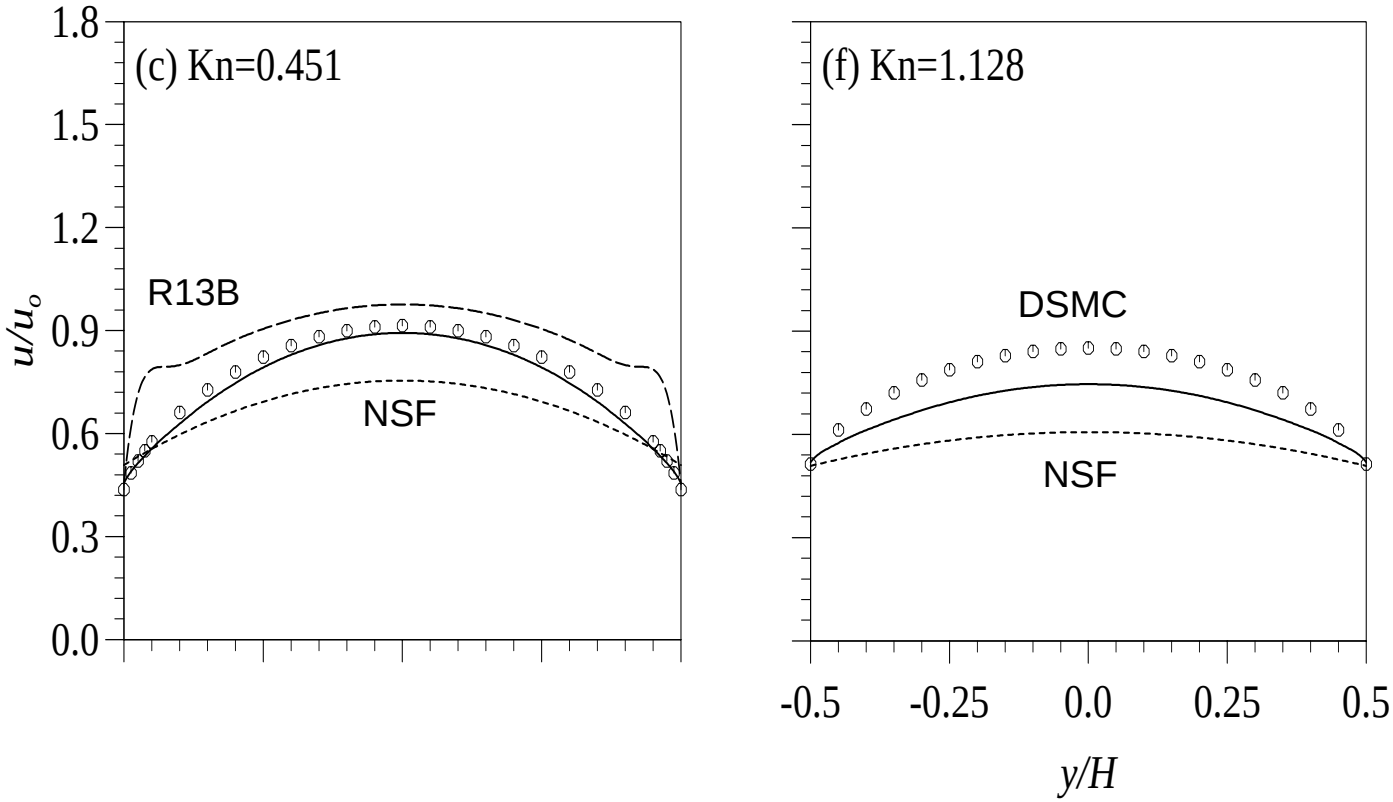

At Kn = 0.451, R13B develops spurious overshoots.

Note overprediction/underprediction by NSF

Some results for Poiseuille flow – Knudsen layer contribution

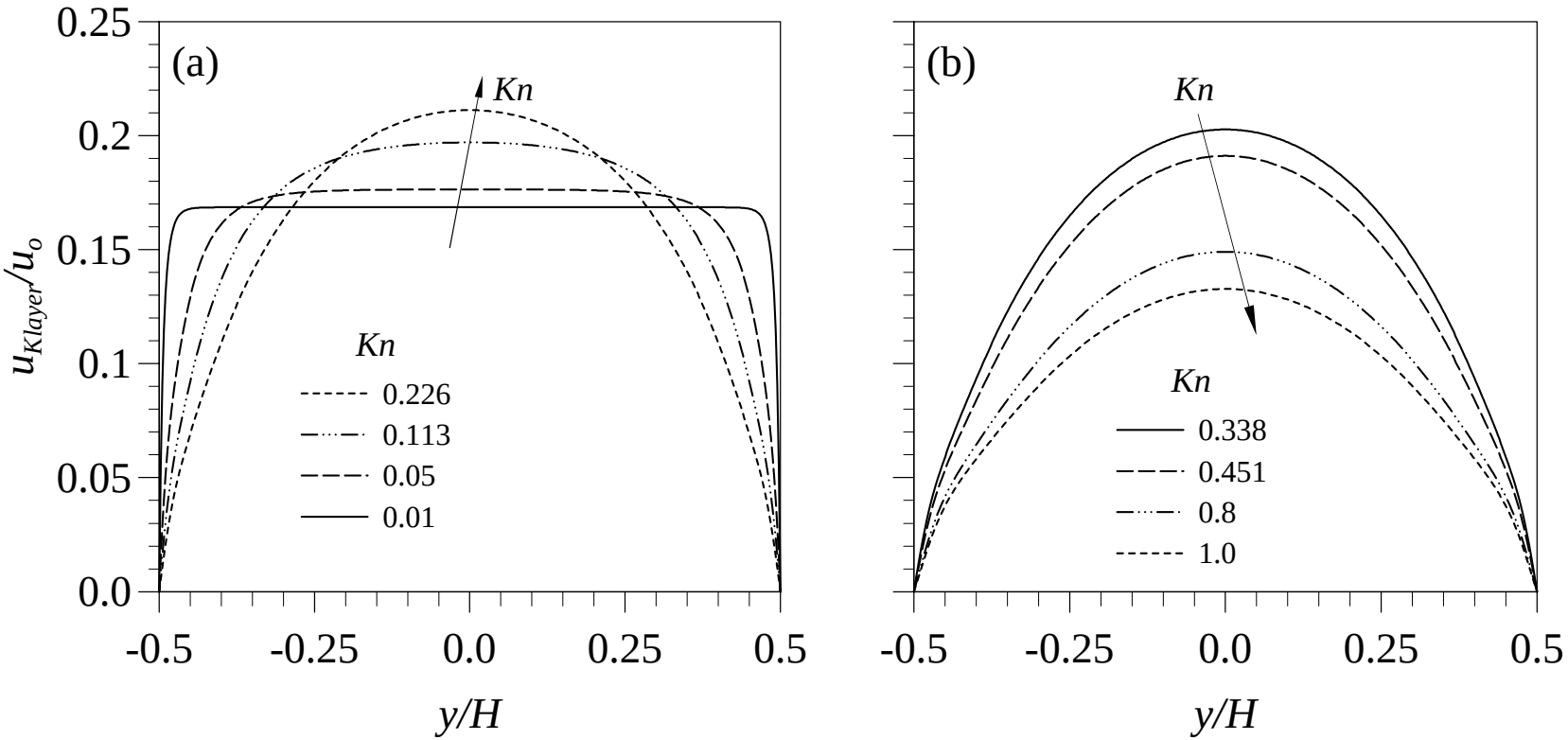

At low Kn, contribution restricted to near-wall and remains constant throughout flow. As Kn increases, Knudsen layers interact and contribution starts to diminish.

Some results for Poiseuille flow

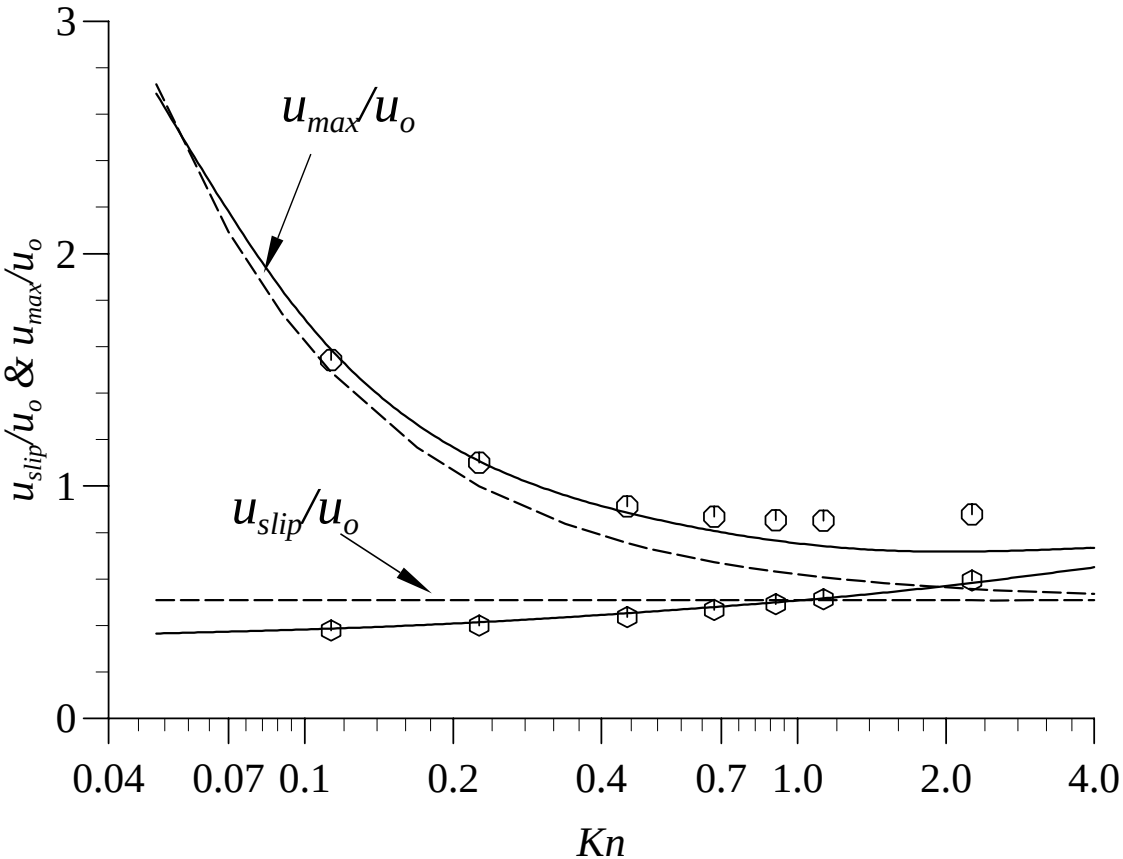

Predicted slip and maximum velocities at different values of Kn.
Symbol: Boltzmann equation (Ohwada *et al*. 1989), solid R26, dashed NSF

Some results for Poiseuille flow – mass flow rate

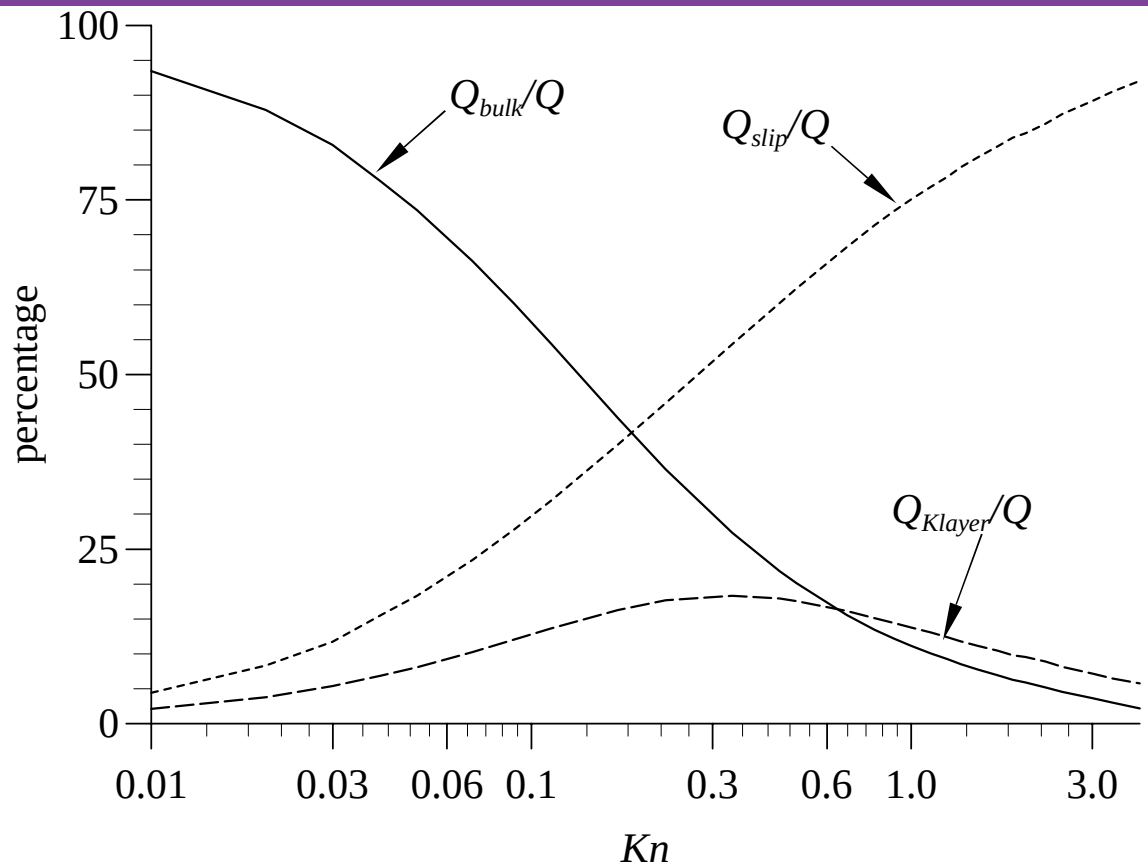

Percentages of mass flow rate contribution to the total mass flow rate from bulk flow, Knudsen layer and slip velocity for the R26 equations

Concluding remarks

- Talk has highlighted some interesting challenges in modelling gas flow in MEMS
- The NSF equations have limited applicability in the slip- and transition-flow regimes
- We have implemented the 26 moment equations and results are promising
- Higher-order systems could be developed (e.g. 48 moment)

Acknowledgements

Special thanks go to:

- Robert Barber (Daresbury)
- Xiaojun Gu (Daresbury)
- Simon Mizzi (Daresbury)
- Jason Reese (Strathclyde)
- Duncan Lockerby (Warwick)
- Rho Shin Myong (Korea)
- Stefan Stefanov (Bulgaria)
- Yonghao Zhang (Daresbury)

Damping

Damping and Kn

- Damping represent a real practical problem for understanding and predicting resonant frequencies of sensors.
- A typical model device is the Tang resonator:
- The resonator consists of a rotor/stator connection
- We need to predict Q factors throughout the Kn regime

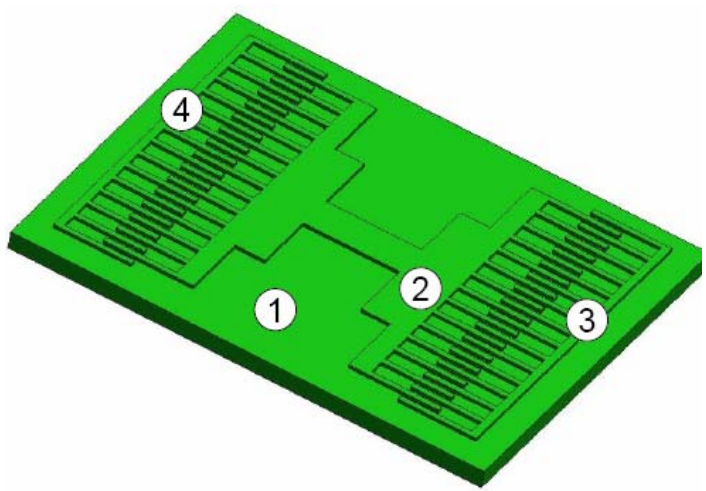

Figure courtesy A. Frangi (Milan)

Damping types

- There are 3 damping effects:
  - Thermoelastic damping (under very low pressures)
  - Squeeze film damping (at the ends)
  - Laterally oscillating damping (Couette flow)

Air damping

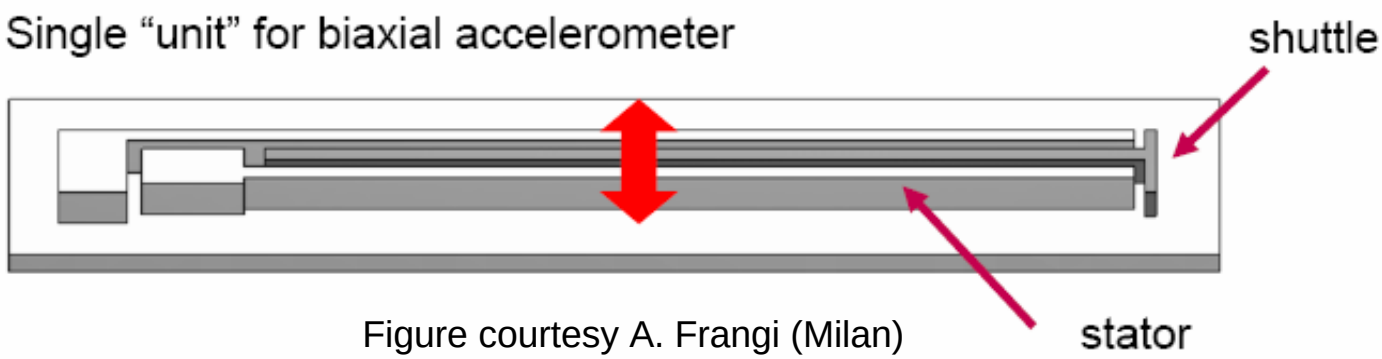

Figure courtesy A. Frangi (Milan)

Damping in slip-flow regime - curvature

Results here are for Stokes' second problem but for a curved surface.

Many resonators are curved and need to understand curvature.

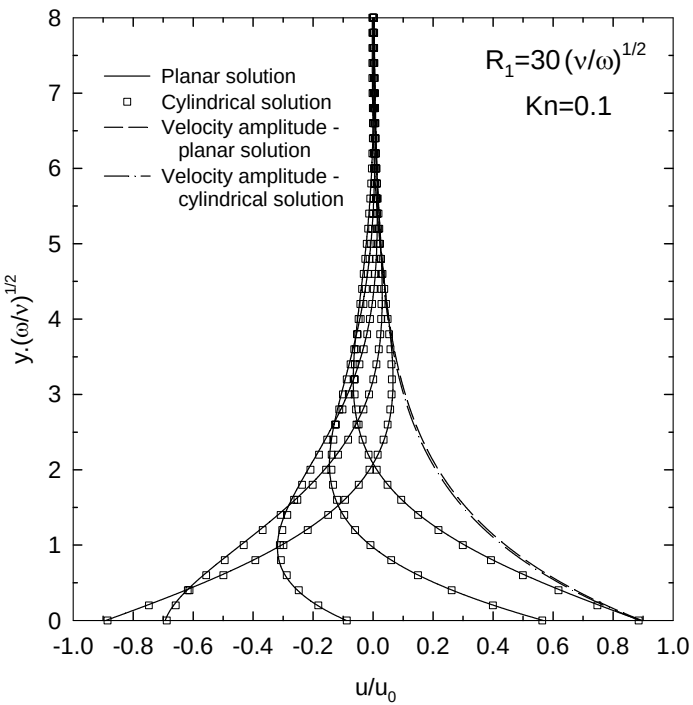

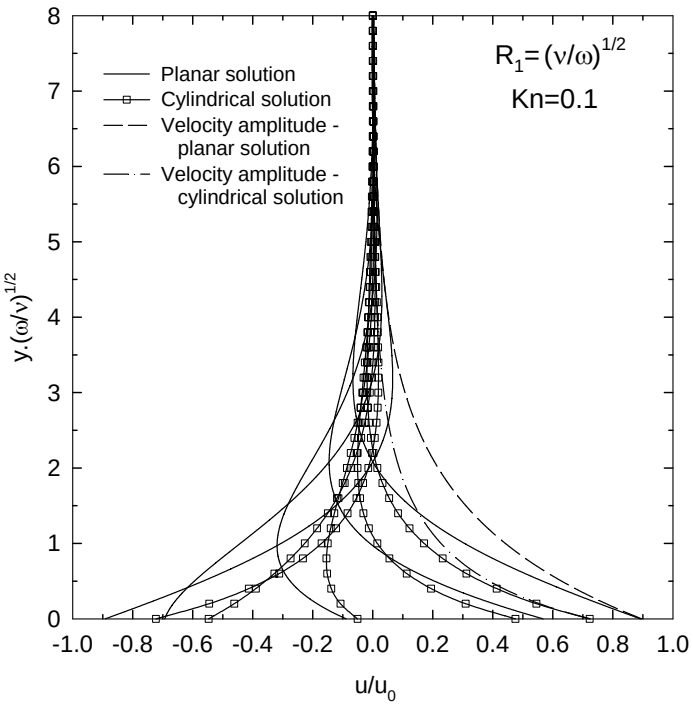

SCAT
SCIENTIFIC COMPUTING ADVANCED TRAINING

ALFA
EUROPEAID
CO-OPERATION OFFICE

First Latin American SCAT Workshop:
Advanced Scientific Computing and Applications

Microfluidics

gas-phase flow at the micro-scale

Prof David Emerson

CCLRC Daresbury Laboratory

University of Strathclyde

CCLRC

University of Strathclyde Glasgow